Published in final edited form as:
Basic Res Cardiol. 2007 September ; 102(5): 369–392. doi:10.1007/s00395-007-0666-z.

Excitation-contraction coupling and mitochondrial energetics

Christoph Maack and
Klinik für Innere Medizin III, Universitätsklinikum des Saarlandes, 66421 Homburg/Saar, Germany, Tel: +49-6841/162-1330, Fax: +49-6841/162-3434, E-Mail: maack@med-in.uni-sb.de

Brian O'Rourke, PhD
Johns Hopkins University, Institute of Molecular Cardiobiology, Division of Cardiology, Baltimore (MD), USA

Abstract

Cardiac excitation-contraction (EC) coupling consumes vast amounts of cellular energy, most of which is produced in mitochondria by oxidative phosphorylation. In order to adapt the constantly varying workload of the heart to energy supply, tight coupling mechanisms are essential to maintain cellular pools of ATP, phosphocreatine and NADH. To our current knowledge, the most important regulators of oxidative phosphorylation are ADP, P_i, and Ca^{2+}. However, the kinetics of mitochondrial Ca^{2+}-uptake during EC coupling are currently a matter of intense debate. Recent experimental findings suggest the existence of a mitochondrial Ca^{2+} microdomain in cardiac myocytes, justified by the close proximity of mitochondria to the sites of cellular Ca^{2+} release, i. e., the ryanodine receptors of the sarcoplasmic reticulum. Such a Ca^{2+} microdomain could explain seemingly controversial results on mitochondrial Ca^{2+} uptake kinetics in isolated mitochondria versus whole cardiac myocytes. Another important consideration is that rapid mitochondrial Ca^{2+} uptake facilitated by microdomains may shape cytosolic Ca^{2+} signals in cardiac myocytes and have an impact on energy supply and demand matching. Defects in EC coupling in chronic heart failure may adversely affect mitochondrial Ca^{2+} uptake and energetics, initiating a vicious cycle of contractile dysfunction and energy depletion. Future therapeutic approaches in the treatment of heart failure could be aimed at interrupting this vicious cycle.

Keywords

calcium; sodium; microdomain; heart failure; adenosine triphosphate; adenosine diphosphate; respiration; tricarboxylic acid cycle

Physiological aspects

The most important function of the heart is to pump blood to supply the body with oxygen and substrates. In order to adapt cardiac output to the constantly changing demand of blood supply, the heart utilizes three major mechanisms to increase cardiac output: the force-frequency relationship (the Bowditch effect or Treppe; [22]), the Frank-Starling mechanism (sarcomere length-dependent activation of contractile force) [66,149,164], and sympathetic activation [28]. All of these mechanisms increase and accelerate myocardial force generation, and at the same time increase cellular energy demand. By these mechanisms, cardiac output during exertion can be increased more than five-fold compared to resting conditions.

Correspondence to: Christoph Maack.

Excitation-contraction coupling

Of fundamental importance for cardiac contraction and relaxation are the processes of excitation-contraction (EC) coupling (Fig. 1). During the action potential (AP), voltage-gated Na^+-channels are activated, and the inward Na^+-current (I_{Na}) induces a rapid depolarization of the cell membrane, facilitating voltage-dependent opening of L-type Ca^{2+}-channels ($I_{Ca,L}$). The Ca^{2+} influx triggers the opening of the ryanodine receptor (RyR2 subtype), inducing the release of even greater amounts of Ca^{2+} from the sarcoplasmic reticulum (SR), a process termed Ca^{2+}-induced Ca^{2+}-release (CICR) [14,15,63,64]. The Ca^{2+} released from RyRs floods the space between the SR and the cell membrane (i. e., the *dyadic* or *junctional cleft*), a gap of typically ~10 nm and covering a volume with a radius of ~200 nm [102,151]. Computational modeling predicted a temporarily and spatially limited increase of the Ca^{2+}-concentration ($[Ca^{2+}]$) in the range from ~10 μM to ~7 mM within the first couple of ms after opening of the RyR2 [14,15,102,133,151,152,158,174,217]. This high junctional $[Ca^{2+}]$ decays rapidly by diffusion into the submembrane space and then further into the bulk cytosol, where it peaks later and at much lower concentrations than in the cleft (at ~1.5 μM in the submembrane space and ~0.5 μM in the bulk cytosol [174,209]). Due to the spatial and temporal heterogeneity of $[Ca^{2+}]$ throughout different compartments of the cytosol, the term of "Ca^{2+} microdomains" was coined [160], with the junctional cleft being the best characterized Ca^{2+} microdomain in cardiac myocytes.

Experimentally, single Ca^{2+} release events can be observed by confocal microscopy as "Ca^{2+} sparks" that occur spontaneously in quiescent cardiac myocytes [42]. These Ca^{2+} sparks arise from the concerted activation of a whole cluster of RyRs [43,177,181]. Ventricular myocytes have a highly organized three-dimensional structure, with invaginations of the plasma membrane reaching into the interior of the cell (Fig. 1). This *transverse tubular* system (*t-tubules*, [182]) facilitates the spatial and temporal coordination of CICR during an AP, resulting in the summation of a large number of Ca^{2+} sparks, whose activation is a stochastic process [31]. In contrast, atrial myocytes lack t-tubules and thus, Ca^{2+}-transients initiate in the periphery of the cell and then spread centripetally [20,110,119]. The increasing cytosolic Ca^{2+} binds to the myofilaments (i. e., troponin C) and induces the contraction of the cell. The contraction of the left and right ventricle leads to the ejection of blood through the aortic and pulmonary valves, respectively, initiating systole. During diastole, relaxation of the myocardium allows passive refilling of the ventricles with blood. Relaxation is initiated by the diffusion of Ca^{2+} from the myofilaments back to the cytosol. The main mechanisms removing Ca^{2+} from the cytosol are the SR Ca^{2+}-ATPase, the sarcolemmal Na^+/Ca^{2+}-exchanger (NCX) and the plasmalemmal Ca^{2+}-ATPase (PMCA) [14,15,179].

Mitochondrial energetics

When the body is at rest, i. e., at normal heart rates of ~60 beats per minute in human, EC coupling already consumes vast amounts of energy. The main cellular energy consumers are the myosin ATPase of the contractile filaments, the plasmalemmal Na^+/K^+-ATPase, and the SR Ca^{2+}-ATPase [15]. It is assumed that ~2% of the cellular ATP pool is consumed in each heart beat, and during maximal workload, the whole ATP pool is turned over within a couple of seconds [7,80,139]. The main sites of energy production are the mitochondria, which take up ~30% of cellular volume [15,222] and are located in close vicinity to the main sites of energy consumption, i. e., the myofilaments, the SR and t-tubules (Figs. 1 and 2; [194,220]). Under physiological conditions, glucose is transformed to pyruvate, which enters mitochondria and is transformed to acetyl-coenzyme A (CoA) by pyruvate dehydrogenase (PDH). Fatty acids are activated to fatty acyl-CoA in the cytosol and transported into mitochondria via the carnitine-acyltranslocase. Acyl-CoA enters β-oxidation, with acetyl-CoA, NADH and $FADH_2$ as the main products. Acetyl-CoA from both glycolysis and β-oxidation enters the tricarboxylic acid (TCA) cycle, resulting in the formation of NADH and $FADH_2$ (Fig. 3A).

NADH feeds electrons into the respiratory chain at complex I (Fig. 4), and succinate enters at complex II. By sequential redox reactions at complexes I–IV, protons are translocated across the inner mitochondrial membrane, establishing a proton gradient (ΔpH) and an electrical gradient ($\Delta\psi_m$) which constitute the proton motive force ($\Delta\mu_H$). The electrons that travel down the respiratory chain are eventually transferred to O_2, forming H_2O. O_2 consumption is respiration. At complex V of the respiratory chain (the F_1/F_0-ATPase), $\Delta\mu_H$ provides the free energy for the generation of ATP from ADP (*oxidative phosphorylation*) [45,187].

Energy supply and demand matching

To tightly orchestrate the enormous energetic flux during the permanent changes of cardiac workload, a highly efficient matching process of energy supply and demand is essential. The two most important regulatory factors identified to date are ADP and Ca^{2+} [7,25,26,37,45, 46,79,129,164,165,194]. The classical respiratory controlhypothesis of Chance and Williams [37] implies that the rate of respiration is regulated by the availability of ADP to the F_1/F_0-ATPase. This is based on the observation that when adding ADP to a suspension of isolated mitochondria, O_2 consumption increases ("state 3 respiration"), and when ADP and/or P_i in the assay are consumed, the rate of respiration decreases again ("state 4 respiration"). However, at the end of the 1980s, a series of experiments by Katz and Balaban et al. [106–108] called into question the regulatory role of ADP for respiration *in vivo*. In isolated rat hearts [106, 107] or instrumented dogs [108] they observed that an increase of cardiac work (by pacing or hormonal stimulation) increased O_2 consumption, however, without any changes of ADP, ATP, P_i or phosphocreatine (PCr). They concluded that respiration is regulated by the (upstream) availability of electrons to the respiratory chain, i. e., the redox state of NADH/ NAD^+, rather than ADP [107,108]. Since NADH is produced by the TCA cycle, and three key enzymes of the TCA cycle (PDH, isocitrate- and α-ketoglutarate dehydrogenases) are activated by Ca^{2+} [53,54,56,57,127,128] (Fig. 3A and B), it was proposed that Ca^{2+} rather than ADP may regulate respiration *in vivo* [106]. In more recent studies, Territo and Balaban et al. extended this concept by showing that besides dehydrogenases, Ca^{2+} also activates the F_1/F_0-ATPase [193,195], and confirmed earlier studies [36] demonstrating that Ca^{2+} increases respiration in less than 100 ms, rapidly enough to support cardiac work transitions *in vivo*.

Of course, Ca^{2+} stimulation of oxidative phosphorylation alone is insufficient to account for the adaptation of mitochondrial energetics to variations in workload induced by changes in muscle length, since these occur largely without variations in the Ca^{2+} transient (metabolic basis of the Frank-Starling law [164]). Furthermore, while Ca^{2+} is able to increase respiration by a factor of ~2, changes of left ventricular filling in isolated perfused rat hearts increases respiration by a factor of more than 10-fold [45,164,194,216]. This has led to other proposed messengers, including P_i [21], although the correlations between this metabolite and cardiac work are also not robust. A difficulty of drawing conclusions regarding the relationship between levels of energy metabolites and ATP production stems from the assumption that bulk measurements of intracellular ATP and P_i (e.g., from NMR measurements) reflect the actual local intramitochondrial concentrations responsible for controlling respiratory flux. This assumption is as weak as assuming that gain of CICR is determined by the bulk cytoplasmic Ca^{2+} concentration. During CICR, bulk cytosolic Ca^{2+} can be completely buffered with no effect of local EC coupling, as demonstrated in studies of "Ca^{2+} spikes" [173,183]. Similarly, cytoplasmic high energy phosphate buffer systems (e.g., creatine kinase (CK) isoenzymes and the rapidly diffusable phosphocreatine, PCr) are present that can limit changes in bulk ATP while shuttling ADP to the mitochondrial adenine nucleotide transporter (ANT), effectively transferring the energetic signal from the site of ATP hydrolysis to the mitochondrion (reviewed in [164]). Hence, in agreement with recent experimental and computational evidence, Ca^{2+}, ADP, and P_i are likely to regulate respiration in a complementary way at sites both upstream and downstream of the respiratory chain, thus providing a balanced availability

of ATP and reduced NADH [25,26,45,46,101,117,164] (see also further below in *Bioenergetic consequences of mitochondrial Ca^{2+}* uptake).

Mitochondrial Ca^{2+} uptake

A prerequisite for Ca^{2+}-induced activation of respiration is that the amount of Ca^{2+} that enters mitochondria is sufficient to activate the dehydrogenases of the TCA cycle. The $K_{0.5}$ for Ca^{2+} activation of the TCA cycle dehydrogenases is in the range of 0.7–1 μM (Fig. 3B; [54, 56,57,127,128]). As reviewed previously [76,77,79,129], Ca^{2+} is taken up by mitochondria via a Ca^{2+} uniporter (mCU; Fig. 1), driven by the large electrochemical gradient for Ca^{2+} across the inner mitochondrial membrane ($\Delta\psi_m \sim -180$ mV). From experiments on suspensions of isolated mitochondria, a half-maximal activation constant ($K_{0.5}$) of ~10–20 μM Ca^{2+} was calculated for mCU-mediated Ca^{2+} transport, yielding a maximum Ca^{2+} flux (V_{max}) of approximately $2 \cdot 10^4$ Ca^{2+} s^{-1} for a single mCU molecule [76,77]. The mCU is inhibited by ruthenium red [124,138,157] or Ru360 [109,117,124], with the latter being more mCU-selective than ruthenium red [124], which also inhibits SR Ca^{2+} release via RyR2 [35]. Furthermore, dissipation of $\Delta\psi_m$ by agents that uncouple respiration (i.e., a combination of FCCP and oligomycin) also inhibits mitochondrial Ca^{2+} uptake by reducing the driving force for Ca^{2+} entry ($\Delta\psi_m$) rather than interacting with the mCU itself.

Recently, Kirichok et al. [109] characterized the mCU by patch-clamping the inner mitochondrial membrane of isolated mitoplasts. Its inwardly rectifying Ca^{2+} current (maximum at $\Delta\psi_m = -160$ mV) had a half-activation constant ($K_{0.5}$) of ~20 mM with a Ca^{2+} carrying capacity that was ~250-fold higher than calculated from experiments on isolated mitochondria ($V_{max} = 5 \cdot 10^6$ Ca^{2+} s^{-1} per single mCU molecule). The current lacked Ca^{2+}-dependent inactivation, but was highly sensitive to ruthenium red and Ru360. The channel density of the mCU at the inner mitochondrial membrane was estimated to amount ~10–40 channels per μm^2, which is only slightly less than the density of voltage-gated Ca^{2+} channels at sarcolemmal membranes of excitable cells (~100 per μm^2; [90,109]). In the absence of Ca^{2+}, the mCU was able to transmit Na^+ (or K^+ to a much smaller degree) instead of Ca^{2+}, but not Mg^{2+}. However, already at low $[Ca^{2+}]_c$ (K_d for Ca^{2+}-*binding* <2 nM), Na^+ and K^+ conductances were completely inhibited. Thus, under physiological conditions in cardiac myocytes ($[Ca^{2+}]_c \approx 100$ nM), the mCU is a highly selective Ca^{2+} channel, allowing Ca^{2+} to accumulate in mitochondria with the least dissipation of $\Delta\psi_m$ [109].

An important difference between the study by Kirichok et al. [109] and previous studies [76, 77] concerning ionic flux estimates is that in mitochondrial suspensions [76,77] or whole cardiac myocytes [222], dissipation of $\Delta\psi_m$ due to Ca^{2+} entry at very high extramitochondrial $[Ca^{2+}]$ may reduce the driving force for further Ca^{2+} uptake, leading to (pseudo-) lower transport rates that saturate at lower extramitochondrial $[Ca^{2+}]$. In contrast, in the study of Kirichok et al. [109], the potential across the inner mitochondrial membrane could be maintained by voltage-clamp, allowing Ca^{2+} flux at much higher extra- and intramitochondrial $[Ca^{2+}]$ than in mitochondrial suspensions or whole cells. This may explain the differences of $K_{0.5}$ and V_{max} for mitochondrial Ca^{2+} transport between those studies [76,77,109].

The primary mitochondrial Ca^{2+} efflux mechanism in cardiac cells is the mitochondrial Na^+/Ca^{2+} exchanger (mNCE) [54,77], which is presumably electrogenic [10,103] by exchanging 1 Ca^{2+} for 3 Na^+, with a K_m for $[Na^+]_i$ of ~8 mM [150]. Earlier studies, however, reported an electroneutral transport mode [48,49].

A mitochondrial Ca^{2+} microdomain

At this point, the question arises as to why the mitochondrial inner membrane expresses a high density of selective Ca^{2+} channels that transport Ca^{2+} primarily at concentrations exceeding

cytosolic bulk [Ca^{2+}] (maximally ~1–3 μmol/L). A possible explanation may be the concept of a *mitochondrial Ca^{2+}-microdomain*, which is already well established in non-cardiac cell types (reviewed by Rizzuto et al. [159,160]). According to this concept, the spatially- and temporally-limited occurrence of very high concentrations of Ca^{2+} ("hot spots") at cellular Ca^{2+}-release sites (e.g., inositol 1,4,5-triphosphate- (IP_3-) receptors of the endoplasmatic reticulum, ER) allows rapid mitochondrial Ca^{2+} uptake despite a relatively low affinity of the mCU for Ca^{2+} [159,160]. On the one hand, this privileged Ca^{2+} signal transmission efficiently adapts cellular energy demand to supply, and on the other hand, it shapes the dynamics of $[Ca^{2+}]_c$ [159,160]. Furthermore, under pathological conditions involving cytosolic Ca^{2+} overload, the low affinity of the mCU may prevent premature mitochondrial Ca^{2+} overload, since the route and rate of cellular Ca^{2+} influx is considerably slower than a triggered release of Ca^{2+} from an intracellular store, i. e., the ER or the SR. Mitochondrial Ca^{2+} overload, together with increased production of reactive oxygen species (ROS), can activate the permeability transition pore (PTP), dissipating $\Delta\psi_m$ and allowing the release of cytochrome c into the cytosol. This can initiate necrotic cell death or, by cytochrome c-dependent activation of cytosolic caspases, apoptosis [29].

Cardiac myocytes, in particular, display a highly organized juxtaposition of sarcolemma, SR and mitochondria (Fig. 2). Mitochondria are ensnared in the SR network and are bounded at each end by the junctional Ca^{2+} release sites (Figs. 1 and 2). Whether this spatial association of mitochondria with the SR results in rapid mitochondrial Ca^{2+} uptake during EC coupling, however, has been highly controversial for over a decade now (for a previous review see Hüser et al. [95]). Over the past 10–15 years, a number of studies have been aimed at elucidating whether during EC coupling, mitochondria take up Ca^{2+} rather slowly, integrating cytosolic Ca^{2+} transients, or rapidly, on a beat-to-beat basis [95]. The clarification of this issue may be of paramount importance to understanding energy supply and demand matching and the interplay between mitochondrial energetics, EC coupling and cellular signaling processes mediated by, e. g., ROS or Ca^{2+} [50]. Thus, in the following discussion, we will review the evidence for and against rapid mitochondrial Ca^{2+} uptake during EC coupling.

Evidence against fast mitochondrial Ca^{2+} uptake

One of the first quantitative estimations of mitochondrial Ca^{2+} uptake during EC coupling comes from a study by Bassani et al. [9]. The aim of that study was to calculate the relative contribution of SR Ca^{2+}-ATPase, NCX, PMCA and mitochondria for cytosolic Ca^{2+} removal after a rapid release of Ca^{2+} from the SR. In rabbit ventricular myocytes loaded with the Ca^{2+}-indicator indo-1/AM, Ca^{2+} was released from the SR by caffeine. Since in the persistent presence of caffeine, the SR Ca^{2+}-ATPase cannot refill the SR, the decay of $[Ca^{2+}]_c$ was achieved primarily by forward-mode I_{NCX}. Consequently, with 0 Na^+ and 0 Ca^{2+} in the extracellular solution (to inhibit I_{NCX}), the decay of $[Ca^{2+}]_c$ was substantially slowed [9]. The remaining decay was attributed to Ca^{2+} removal by mitochondria and the PMCA, since it was blocked by mitochondrial uncoupling (by application of FCCP and oligomycin 5 s prior to the caffeine pulse) or inhibition of PMCA, each contributing about equally to the Ca^{2+} removal rate [9]. Thus, the relative contributions of SR Ca^{2+}-ATPase, NCX, PMCA and mitochondria to diastolic Ca^{2+}-removal in rabbit ventricular myocytes were 70%,28%,1% and 1% [9,14, 15].This implies that under steady-state conditions, 70% of Ca^{2+} cycle into and out of the SR, whereas ~29% enter the cell via L-type Ca^{2+} channels and leave the cell via the NCX and PMCA. Consequently, only 1% of Ca^{2+} would enter and leave mitochondria on every beat. This was in agreement with estimates by Sipido and Wier [179] and the conception that the affinity of the mCU for Ca^{2+} transport was too low to allow beat-to-beat oscillations of mitochondrial $[Ca^{2+}]$ ($[Ca^{2+}]_m$) during cytosolic Ca^{2+} transients [14,15].

In the following years, a number of studies attempted to measure mitochondrial Ca^{2+} uptake during EC coupling more directly, with quite controversial results [12,26,33,59–61,68,72–74,100,117,119,136,137,140,141,144,147,148,161,170,171,176,191,200,201,213]. One reason for these controversial results may be that different techniques were employed to investigate the kinetics of mitochondrial Ca^{2+}-uptake. It is a technical challenge to reliably and selectively monitor changes in $[Ca^{2+}]_m$ without contamination by cytosolic Ca^{2+} signals. In most approaches, cell-permeable fluorescent Ca^{2+} indicators (e.g., indo-1/AM [59,60,72–74,221,222], rhod-2/AM [26,117,119,148,176,191,200,201] or fluo-3 [33,144,170]) penetrate sarcolemmal and mitochondrial membranes and accumulate (to different degrees) in the mitochondrial matrix. To avoid contamination of the fluorescence signal by cytosolic Ca^{2+}, the groups of Hansford, Silverman [59,60,74,136,137] and Bers [26,222] applied $MnCl_2$ in the extracellular solution. Mn^{2+} enters the cell, presumably via L-type Ca^{2+}-channels, binds to cytosolic indo-1 with ~20-fold higher affinity than Ca^{2+} and quenches its fluorescence [123,137,222]. Although Mn^{2+} competes with Ca^{2+} for the mCU [69,123], and thus can be taken up into mitochondria as well [26,222], it was proposed that at the concentrations used, cytosolic free Mn^{2+} was too low to effectively compete with Ca^{2+} for the mCU, since most cytosolic Mn^{2+} should be bound to indo-1 [222]. Indeed, $MnCl_2$ did not affect cell shortening, indicating that despite a potential inhibitory effect of Mn^{2+} on $I_{Ca,L}$ [123], EC coupling was not hampered [137]. Depending on the loading protocol of indo-1/AM, $MnCl_2$ reduced its overall fluorescence by ~30–55%, indicating that ~45–70% of fluorescence stemmed from non-cytosolic compartments, i. e., primarily from mitochondria [137,222].

In all studies using the Mn^{2+}-quench method [59,60,74,136,137], no beat-to-beat oscillations of $[Ca^{2+}]_m$ in response to cytosolic Ca^{2+}-transients could be detected (Fig. 5A and B). Instead, a slow, cumulative increase of $[Ca^{2+}]_m$ from resting levels (~90 nmol/L) to ~400–600 nmol/L was observed in response to β-adrenergic stimulation and an increase of stimulation frequency to 4 Hz (Fig. 5C; [60,137]). When cells were paced at 0.2 Hz, lowering of extracellular $[Na^+]$ induced reverse-mode I_{NCX}-dependent cytosolic Ca^{2+}-influx with subsequent slow mitochondrial Ca^{2+}-accumulation [137]. Plotting $[Ca^{2+}]_m$ against the respective $[Ca^{2+}]_c$ (determined in a different set of cells) revealed a nonlinear relationship between $[Ca^{2+}]_m$ and $[Ca^{2+}]_c$, with a threshold at $[C^{2+}]_c \approx 500$ nmol/L and an exponential increase of $[Ca^{2+}]_m$ above this threshold (Fig. 5D; [137]). This exponential relationship indicates positive cooperativity of mitochondrial Ca^{2+} uptake, a phenomenon observed also in whole cardiac myocytes [67,222], isolated mitochondria [126,129] and other cell types [44]. The exponential slope was heavily influenced by extramitochondrial $[Na^+]$ [45,126,129], reflecting the critical influence of mNCE activity on steady-state levels of $[Ca^{2+}]_m$. Mitochondrial Ca^{2+}-uptake was sensitive to the mCU-inhibitors ruthenium red or Ru360, or dissipation of $\Delta\psi_m$ [60,137], whereas mitochondrial Ca^{2+}-decay was reduced by the mNCE-inhibitors clonazepam or CGP-37157 [74].

In an elaborate study on indo-1/AM loaded myocytes, Zhou et al. [222] used different approaches involving Mn^{2+}-quenching, patch-clamping with whole cell dialysis and measurement of cell shortening as a biosensor for $[Ca^{2+}]_c$ to determine the kinetics of mitochondrial Ca^{2+} uptake at physiological $[Ca^{2+}]_c$ in ferret and cat cardiac myocytes. $[Ca^{2+}]_c$ was increased by voltage steps from −40 to +110 mV, inducing a relatively slow I_{NCX}-induced Ca^{2+} influx that lasted several seconds. In response to cytosolic Ca^{2+} transients, there was no detectable increase of $[Ca^{2+}]_m$ as long as resting $[Ca^{2+}]_c$ was below a threshold of ~300–500 nM [222]. However, above 500 nmol/L, a similar absolute change of $[Ca^{2+}]_c$ did increase $[Ca^{2+}]_m$, confirming the threshold phenomenon and positive cooperativity of the mCU described before [44,45,126,129,137]. Since $[Ca^{2+}]_m$ followed $[Ca^{2+}]_c$ with a lag of ~1 s and a maximum flux across the mCU of ~10 μM/s, it was concluded that in agreement with the studies by Miyata et al. [137] and Di Lisa et al. [60], this flux would be too small to allow mitochondrial beat-to-beat Ca^{2+}-transients during EC coupling.

Although myocyte shortening and thus, the processes of EC coupling were minimally affected by Mn^{2+}-treatment [60,137], it cannot be ruled out completely that mitochondrial Ca^{2+}-uptake was affected by Mn^{2+} to some extent. Mn^{2+} competes with Ca^{2+} for the mCU [76,77] (although patch-clamp studies suggest that the selectivity of the mCU for Ca^{2+} vs Mn^{2+} is > 15-fold [109]) and can be taken up into mitochondria as well [26,33,69,76,77,222], where it may inhibit oxidative phosphorylation [70]. Thus, Mn^{2+} could potentially reduce the rate of the mCU, on the one hand by competing with Ca^{2+}, on the other hand by reducing $\Delta\psi_m$. Furthermore, Mn^{2+} might quench mitochondrial indo-1 [222]. Finally, the mNCE is inhibited by Mn^{2+} as well [69,76,77,137], which could affect Ca^{2+} efflux kinetics. To avoid these undesired effects of $MnCl_2$, Griffiths et al. [73], who had previously used the Mn^{2+}-quench method [74], developed the "heat treatment" protocol, in which incubation of indo-1/AM loaded cardiac myocytes at 25 °C for 2.5 h and 37 °C for 1.5 h promoted the loss of cytosolic indo-1 through probenecid-sensitive plasma membrane anion pumps [73]. With this technique, a similar behavior of $[Ca^{2+}]_m$ as after $MnCl_2$-treatment was observed in rat myocytes, i. e., no beat-to-beat transients, but a cumulative increase of $[Ca^{2+}]_m$ [73]. Interestingly, in a follow-up study using the same heat treatment protocol on indo-1 loaded myocytes, Griffiths [72] reported that in guinea-pig, but not rat cardiac myocytes, beat-to-beat $[Ca^{2+}]_m$ transients could be observed, suggesting that species-dependent differences of mitochondrial Ca^{2+} uptake may exist.

More support for slow mitochondrial Ca^{2+} uptake comes from a very recent study by Sedova et al. [170], who determined $[Ca^{2+}]_m$ by incubating cells with fluo-3, which localized primarily to mitochondria. To eliminate cytosolic traces of fluo-3, the cell membrane was permeabilized with digitonin, and cells dialyzed with a Ca^{2+}-free "intracellular" solution. To simulate cytosolic Ca^{2+} transients, cells were exposed to rapid ejections of a Ca^{2+} holding solution (up to 100 μM) from a micropipette into the bath solution, yielding a peak $[Ca^{2+}]$ of ~5 μM in the cytosol. To prevent cells from contracting, 2, 3-butanedione monoxime (BDM) was applied. Under these conditions, no beat-to-beat transients of $[Ca^{2+}]_m$ could be observed. Nevertheless, mitochondria accumulated Ca^{2+} in a ruthenium red- and FCCP-sensitive manner as extramitochondrial Ca^{2+} ($[Ca^{2+}]_{em}$) was raised above 500 nM, with a $K_{0.5}$ of 4.4 μM $[Ca^{2+}]_{em}$, again confirming the phenomenon of a threshold for mitochondrial Ca^{2+} uptake [44,45,126,129,137,222]. Interestingly, elevation of $[Na^+]$ from 0 to 40 mM decreased the velocity and amplitude of (slow) mitochondrial Ca^{2+} uptake by about half, indicating that net $[Ca^{2+}]_m$ was critically governed by the equilibrium between mCU and mNCE kinetics, even if the mNCE is manyfold slower than the mCU.

Although highly elegant in design, a potential disadvantage of the study by Sedova et al. [170] could be that cytosolic Ca^{2+} transients were simulated by *extracellular* application of high $[Ca^{2+}]$. This may neglect to some extent the spatio-temporal aspects of EC coupling, including the potential existence of a mitochondrial Ca^{2+} microdomain. Furthermore, BDM inhibits respiration at complex I [167] and could thus affect the electrochemical driving force for mitochondrial Ca^{2+} uptake.

Evidence for fast mitochondrial Ca^{2+} uptake

The first experimental evidence for rapid mitochondrial Ca^{2+} uptake in intact cardiac myocytes comes from the group of Wendt-Gallitelli and Isenberg [100,213]. By performing electron-probe microanalysis (EPMA) after shock freezing guinea-pig cardiac myocytes at different time points of a voltage-clamp-induced cytosolic Ca^{2+} transient, they observed a mitochondrial Ca^{2+} transient that peaked ~15–20 ms after the cytosolic transient [213]. This technique, however, allowed determination of total, but not free $[Ca^{2+}]$ in the respective compartments. According to their calculations, total $[Ca^{2+}]_m$ rose from 0.5 to 1.3 mmol/kg dry weight within ~45 ms, yielding a flux of ~100 nmol/s/mg protein across the mCU. Thereafter, $[Ca^{2+}]_m$ decayed back to ~1.3 mmol/kg dry weight within ~400ms with a rate of ~36 nmol/s/mg protein

[100]. These values were ~2 orders of magnitude greater than results from isolated mitochondria [76,77,79,129]. Interestingly, a mitochondrial Na^+ transient was observed with a delay of ~55 ms after the mitochondrial Ca^{2+} transient, indicating that matrix Ca^{2+} was rapidly replaced by Na^+ via the mNCE [100]. The decay of matrix $[Na^+]$ is explained by exchange of Na^+ against H^+ via the Na^+/H^+-exchanger (mNHE), which dissipates the proton motive force ($\Delta\mu_H$) and thus, $\Delta\psi_m$ (Fig. 1) [77,79,129].

In a different set of experiments, Isenberg et al. [100] performed patch-clamp experiments in guinea-pig myocytes in which $[Ca^{2+}]_c$ was determined by indo-1 salt that was introduced via the patch pipette. Cytosolic Ca^{2+} transients were induced by voltage-clamping in the absence and presence of mitochondrial uncouplers to inhibit the mCU. In the presence of the uncouplers, an ~50% increase of the amplitude of the cytosolic Ca^{2+} transient was observed for ~1–3 min. By subtracting the cytosolic Ca^{2+} transient in the absence from the one in the presence of uncouplers, they obtained an indirect estimate of a mitochondrial Ca^{2+} transient. It has to be taken into account though that when elevating $[Ca^{2+}]_c$ by blocking mitochondrial Ca^{2+} uptake, allosteric Ca^{2+}-activation of I_{NCX} [118,208] or Calmodulin (CaM) kinase II dependent phosphorylation of phospholamban (PLB) and subsequent increase of SR Ca^{2+}-ATPase activity [15,120] could have accelerated cytosolic Ca^{2+} decay. This may, in turn, overestimate the rate of decay of $[Ca^{2+}]_m$ derived from the indirect mitochondrial Ca^{2+} transient [100]. Furthermore, it should be considered that uncoupling of mitochondrial respiration is problematic since a number of important factors involved in EC coupling (ATP, sarcolemmal K_{ATP} current, $\Delta\psi_m$, cellular redox state etc.) change in response to uncouplers, which may hamper the interpretation of data. Nevertheless, the data for the first time suggested that cardiac mitochondria take up Ca^{2+} rapidly enough to shape cytosolic Ca^{2+} transients.

In contrast to the results of Isenberg et al. [100,213], Moravec and Bond [140,141] were unable to detect mitochondrial Ca^{2+} transients using a similar technique (EPMA). However, instead of single guinea-pig myocytes, they used hamster papillary muscles. In this context it may be important to consider that also Di Lisa et al. [59,60] were unable to observe beat-to-beat $[Ca^{2+}]_m$ transients in hamster myocytes, again raising the question of potential species-differences, as suggested by Griffiths [72]. Another possible explanation for differential results comes from a follow-up study of the Isenberg group [68] on guinea pig myocytes, where Ca^{2+} and Na^+ rapidly increased in response to cytosolic Ca^{2+} transients in peripheral, but not in central mitochondria.

A series of studies from the Lemasters group [33,144,200,201] investigated mitochondrial Ca^{2+} uptake by confocal microscopy in fluo-3/AM [33,144]-, rhod-2/AM- [200,201] and indo-1/AM [144] loaded rabbit cardiac myocytes. In their first study [33], cytosol and mitochondria were equally loaded with fluo-3, and it was assumed that by high spatial resolution, cytosolic and mitochondrial signals were collected specifically without spill-over from the respective other compartment. In the other studies [144,200,201], a cold/warm loading protocol was performed to enhance mitochondrial accumulation of the respective dye. Mitochondrial localization was verified by colocalization of fluo-3 signals with fluorescence from tetramethylrhodamine methyl ester (TMRM), a potentiometric dye that localizes to mitochondria and is an indicator of $\Delta\psi_m$, or rhodamine 123 [33,144]. Using this technique, rapid mitochondrial Ca^{2+} transients were observed, with more or less similar kinetics as cytosolic Ca^{2+} transients. β-Adrenergic stimulation increased amplitudes of both cytosolic and mitochondrial Ca^{2+} transients [33,144]. In one study [144], quantification of mitochondrial Ca^{2+} transients with indo-1/AM revealed an increase of $[Ca^{2+}]_m$ from ~200 nmol/L during diastole to 500 or 700 nmol/L during systole in the absence and presence of β-adrenergic stimulation, respectively [144]. In the most recent study [200], $[Ca^{2+}]_c$ and $[Ca^{2+}]_m$ were measured by simultaneous recordings of (cytosolic) fluo-3 and (mitochondrial) rhod-2

fluorescence. The specific localization was verified by inhibiting mitochondrial, but not cytosolic Ca^{2+} transients with the mCU-inhibitor ruthenium red [200].

Due to the relatively low temporal resolution in these studies, no discrimination of cytosolic and mitochondrial Ca^{2+} kinetics could be obtained. Another potential disadvantage is that the spatial resolution of a confocal microscope (~0.9–1.2 μm) may not be high enough to detect fluorescence exclusively from a single mitochondrion and thus, contamination of the mitochondrial signal by cytosolic dye may occur [95], especially when considering that myocytes move during a twitch, and no attempts were made to eliminate signal contamination by cytosolic dye. On the other hand, the fact that mitochondrial, but not cytosolic Ca^{2+} transients were inhibited by ruthenium red [200] indicates that rhod-2 and fluo-3 monitored Ca^{2+} quite selectively from the respective compartments.

To avoid contamination of mitochondrial Ca^{2+}-signals with cytosolic traces of a Ca^{2+}-indicator, we recently developed a technique (modified from the approach of Zhou et al. [222]) in which we first loaded adult guinea-pig myocytes with cell-permeable rhod-2/AM, and then patch-clamped these cells in order to wash out cytosolic traces of rhod-2 by whole-cell dialysis [117]. At the same time, the cell-impermeable Ca^{2+}-indicator indo-1 (penta-K^+ salt) was introduced via the patch pipette. This allowed us to specifically monitor $[Ca^{2+}]_c$ and $[Ca^{2+}]_m$ within the same cell. Using a voltage-clamp protocol, we induced cytosolic Ca^{2+} transients by step depolarizations from −80 to + 10 mV at different frequencies. The main results were that with every cytosolic Ca^{2+} transient, a rapid mitochondrial Ca^{2+} transient occurred, its amplitude (Δ) linearly correlating with the amplitude of $\Delta[Ca^{2+}]_c$ (Fig. 6A–D). In contrast to most previous studies [33,68,72,100,144,161,200,201,222], the upstroke of $[Ca^{2+}]_m$ *preceded* the upstroke of $[Ca^{2+}]_c$ by several ms, whereas the decay of $[Ca^{2+}]_m$ was ~2.5-fold slower than of $[Ca^{2+}]_c$. In response to β-adrenergic stimulation or an increase of stimulation frequency, this led to a stepwise accumulation of diastolic $[Ca^{2+}]_m$ (Fig. 6A–D). Mitochondrial Ca^{2+}-uptake could be inhibited by intracellular application of Ru360 (Fig. 6F), and the Ca^{2+}-decay was slowed by CGP-37157 [117]. A drawback of our study is that since $[Ca^{2+}]_m$ was determined by rhod-2, which is not a ratiometric dye as indo-1, no direct quantification of $[Ca^{2+}]_m$ was obtained.

A whole different approach to circumvent cytosolic contamination with Ca^{2+}-indicators was chosen by Robert et al. [161], who transfected neonatal cardiac myocytes with the Ca^{2+}-sensitive photoprotein aequorin, specifically targeted to the cytosol or mitochondria, respectively. With this technique they also observed beat-to-beat oscillations of $[Ca^{2+}]_c$ and $[Ca^{2+}]_m$ in spontaneously contracting neonatal myocytes (~1 Hz), with $[Ca^{2+}]_c$ peaking after 50–100 ms, and $[Ca^{2+}]_m$ peaking with ~50 ms delay. The Ca^{2+} decay was ~100–150 ms slower in mitochondria than in the cytosol. In response to increasing extracellular $[Ca^{2+}]$ or β-adrenergic stimulation, an increase of amplitude and/or frequency of Ca^{2+}-oscillations was observed in both compartments. Similar results were obtained with the green fluorescent protein- (GFP-) based fluorescent Ca^{2+}-indicator "ratiometric-pericam" [161]. Bell et al. [12], recently used this technique in *adult* rat cardiac myocytes, which were adenovirally infected with targeted aequorin to selectively monitor $[Ca^{2+}]_c$ and $[Ca^{2+}]_m$. Agreeing with the results on neonatal cells [161], they observed beat-to-beat oscillations of $[Ca^{2+}]_c$ and $[Ca^{2+}]_m$ during electrical field stimulation. $[Ca^{2+}]_m$ increased simultaneously with $[Ca^{2+}]_c$, but decreased more slowly [12]. The strength of these studies [12,161] is the compartmental specificity of the Ca^{2+}-signals, which was illustrated by permeabilization experiments. However, a disadvantage is the relatively low signal-to-noise ratio of the fluorescence signals that necessitates the recording of a whole optical field with multiple cardiac myocytes.

Evidence for a mitochondrial Ca^{2+} microdomain

To functionally address whether rapid mitochondrial Ca^{2+} uptake is achieved due to a mitochondrial Ca^{2+} microdomain, Sharma et al. [176] and Szalai et al. [191] loaded rat cardiac myocytes or cardiac myotubes (H9c2 cells) with rhod-2/AM and eliminated cytosolic dye by chemical membrane permeabilization. $[Ca^{2+}]_c$ or perimembrane $[Ca^{2+}]$ were monitored by dialyzing the per-meabilized cells with fura-2 salt or fura-2 C18, respectively. Application of caffeine induced rapidly increasing Ca^{2+} transients in both the cytosol and mitochondria, with the decay of $[Ca^{2+}]_m$ being slower than of $[Ca^{2+}]_c$. Interestingly, when buffering $[Ca^{2+}]_c$ with BAPTA or EGTA [191], cytosolic, but not mitochondrial Ca^{2+} transients were inhibited, suggesting that either the size of the Ca^{2+}-complexing molecules or their Ca^{2+}-complexing kinetics prevented buffering of highly localized and short-lived increases of $[Ca^{2+}]$ in the space between RyR2 and mCU (hot spots; Fig. 1 and 2).

Furthermore, a more *rapid* increase of $[Ca^{2+}]_c$ facilitated a greater increase of $[Ca^{2+}]_m$ compared to a *slower* increase of $[Ca^{2+}]_c$ with similar amplitude, indicating that the *rate* of SR Ca^{2+} release has an important impact on mitochondrial Ca^{2+} uptake [176]. To match the velocity of mitochondrial Ca^{2+} uptake after caffeine-induced SR Ca^{2+} release, a $[Ca^{2+}]$ of ~30 μM had to be established in the cytosol of permeabilized cells, suggesting that the local $[Ca^{2+}]_c$ around the mCU may be several-fold higher than in the bulk cytosol, where it peaks at ~1–2 μmol/L (Fig. 7). The steep part of the concentration-response curve between 10 and 30 μmol/L (Fig. 7B) is in agreement with the $K_{0.5}$ of the mCU for Ca^{2+} transport determined in isolated mitochondria (10–20 μM; [54,76,77]). In a parallel study from the lab of Hajnoczky, Pacher et al. [147] calculated that ~26% of the Ca^{2+} released from the SR after caffeine-exposure was taken up by mitochondria. This contrasts to the 1% of Ca^{2+} removed by mitochondria after SR Ca^{2+} release as calculated by Bassani et al. [9].

To test the existence of a mitochondrial Ca^{2+} microdomain *in silico*, we used a computer model that integrates the kinetics of mitochondrial Ca^{2+} handling (i. e., mCU and mNCE), the TCA cycle and oxidative phosphorylation [45]. Pulses of Ca^{2+} resembling those expected to be encountered in a mitochondrial Ca^{2+}-microdomain [174,176,191] ($[Ca^{2+}]_{MD}$) were simulated with an exogenous Ca^{2+} spike function with peak $[Ca^{2+}]$ of either 10 or 20 μM for a duration of 50 ms (Fig. 8D). These pulses of $[Ca^{2+}]_{MD}$ elicited rapid $[Ca^{2+}]_m$ transients with slow decay. An increase of either $[Ca^{2+}]_{MD}$ amplitude (Fig. 8A) or frequency (Fig. 8B) independently increased diastolic $[Ca^{2+}]_m$. An increase in both amplitude *and* frequency of the pulses potentiated diastolic $[Ca^{2+}]_m$ accumulation (Fig. 8C). These simulations were in qualitative agreement with experimental results [12,117,144,161] and lend support to the hypothesis that mitochondria sense $[Ca^{2+}]$ in a microdomain, rather than the bulk $[Ca^{2+}]_c$.

Implications of rapid mitochondrial Ca^{2+} uptake for EC coupling

Several studies indicate that by buffering $[Ca^{2+}]_c$, rapid mitochondrial Ca^{2+} uptake directly affects EC coupling [61,100,117,119,124,147,148,171]. When blocking mitochondrial Ca^{2+} uptake, an increase of cytosolic Ca^{2+} transients was observed (Fig. 6E and F; [100,117,124, 171]). It also appears that the highly organized pattern of mitochondria localized close to the SR provides a "local control" of SR Ca^{2+} release events. In cardiac myotubes, spontaneous Ca^{2+} release events restricted to a small number of RyRs (Ca^{2+} sparks) elicited miniature mitochondrial matrix Ca^{2+} signals (Ca^{2+} *marks*) that lasted less than 500 ms [148] and roughly resembled the kinetics of mitochondrial Ca^{2+} uptake and release kinetics recorded under steady-state conditions during whole-cell cytosolic Ca^{2+} transients (Fig. 6D; [12,117]). Accordingly, localized Ca^{2+} sparks induced transient focal depolarizations of $\Delta\psi_m$ by ~10–15 mV [61]. The propagation of caffeine-induced Ca^{2+} sparks was suppressed by mitochondria, since inhibition of the mCU (with Ru360) resulted in regenerative Ca^{2+} waves across the whole cell [171]. Similarly, in atrial myocytes, where cytosolic Ca^{2+} transients occur primarily in the

periphery due to the lack of t-tubules, uptake of Ca^{2+} into mitochondria and the SR prevented the propagation of the peripheral Ca^{2+} transients to more central parts of the cell [119], even though the density of mitochondria is lower in atrial than in ventricular cells [171]. Taken together, these results suggest that mitochondria may function as spatial buffers for Ca^{2+}, regulating the propagation of Ca^{2+} release events and thus, contractility of the cell. However, regarding the controversy on the amount of Ca^{2+} taken up by mitochondria during EC coupling [9,117,147], the definite relevance of mitochondrial Ca^{2+} uptake for cytosolic Ca^{2+} homeostasis is still incompletely understood.

Molecular identity of the mCU

So far, the mCU has been characterized functionally, but not on a molecular level. Thus, most studies rely on the mCU's sensitivity to Ru360 or ruthenium red. Sparagna et al. [186] observed a rapid mode of uptake, termed RaM, that allowed rapid mitochondrial Ca^{2+} uptake typically at the *first* of a series of Ca^{2+} pulses in liver mitochondria. The RaM was less sensitive to ruthenium red than the mCU. However, in cardiac mitochondria, the RaM required > 30 s to become fully reactivated at extramitochondrial $[Ca^{2+}] < 100$ nmol/L [30] and thus, cannot be responsible for beat-to-beat mitochondrial Ca^{2+} uptake. Furthermore, Beutner et al. [18,19] have proposed that mitochondrial RyR (RyR1 subtype) channels may mediate Ca^{2+} flux across the inner mitochondrial membrane. The binding of [^{3}H]ryanodine to this mRyR1 has a bell-shaped Ca^{2+}-dependence, with an optimum between 10–30 μM [19], the latter value comparable to the reported $K_{0.5}$ of the mCU for Ca^{2+} [54,77]. Currently, there is no specific inhibitor that could differentiate between the mCU and mRyR1. Ruthenium red inhibits the mCU [124], but also the mRYR1 [19] and the RyR2 subtype [124]. In contrast, Ru360 inhibits the mCU, but not the RyR2 subtype [124]. However, whether the mRyR1 is inhibited by Ru360 has not been determined [19]. Thus, it may be possible that the mRyR1 contributes to mitochondrial Ca^{2+}-uptake, or may even resemble the mCU.

Bioenergetic consequences of mitochondrial Ca^{2+} uptake

A series of studies by Brandes and Bers [23–27] provided important insights into the physiological role played by mitochondrial Ca^{2+} uptake with respect to the regulation of respiration. In isolated rat cardiac trabecule loaded with rhod-2/AM, $[Ca^{2+}]_m$ and NADH were determined in response to an abrupt change of workload (Fig. 9A; [26]). When increasing stimulation frequency from 0.5 to 2 Hz, a rapid initial oxidation of NADH occurred (*undershoot*). This oxidation was attributed to pronounced ATP hydrolysis resulting in an increase of ADP, which stimulated ATP-generation at the F_1/F_0-ATPase [25]. Since ATP synthesis is associated with dissipation of $\Delta\psi_m$, more electrons need to be donated by NADH to the respiratory chain to maintain $\Delta\psi_m$ (Fig. 4). After the initial oxidation, a phase of slow NADH *recovery* was observed, which reached a new steady state after several seconds. The time course of NADH recovery was closely associated with the accumulation of $[Ca^{2+}]_m$ (Fig. 9A, lower panel), and thus related to Ca^{2+}-induced stimulation of TCA cycle dehydrogenases [26]. After returning to 0.5 Hz stimulation frequency, an *overshoot* of NADH was observed, which is explained by maintained elevation of TCA cycle dehydrogenase activities despite decreased ADP-stimulated respiration [26]. NADH again slowly recovered towards baseline levels in parallel to the decay of $[Ca^{2+}]_m$.

Similar results were obtained in isolated cardiac myocytes (Fig. 9B; [101,117]), albeit with different relative amounts of the initial oxidation- and the secondary recovery phases, respectively. These differences may be related to the fact that in prestretched cardiac trabeculae [26], work during contraction may be severalfold higher than in unstretched single myocytes. Thus, ADP-related oxidation of NADH was less pronounced in single cells [101,117], whereas the Ca^{2+}-dependent NADH recovery was comparable between trabeculae [26] and single cells [101,117], resulting in net reduction of the NADH/NAD^+ pool after increasing stimulation

frequency in single cells (Fig. 9B; [101,117]). Jo et al. [101] corroborated the concept that NADH oxidation at the onset of work is related to ADP-induced stimulation of respiration, since addition of ADP or P_i oxidized NADH in permeabilized myocytes. Furthermore, the NADH recovery phase was inhibited by blocking mitochondrial Ca^{2+} uptake with Ru360 [101] during electrical stimulation, confirming the Ca^{2+}-dependence of this process. In an earlier set of studies, White and Wittenberg [214,215] had observed that in response to 5 Hz stimulation, NADH was oxidized at 95% O_2, whereas it was reduced at 20% O_2. They concluded that if O_2 availability limits the rate of respiration (i. e., at 20% O_2), then the equilibrium of the NADH/NAD^+ redox potential is shifted towards NADH reduction by Ca^{2+}-stimulated TCA cycle dehydrogenases, and away from respiratory chain-induced oxidation [214,215].

The transient behavior of NADH determined experimentally [23,25,26,101,117,214,215] could be reproduced by computational modeling in different studies [45,46,101]. In our recent model that integrates the processes of EC coupling and mitochondrial bioenergetic responses of the cardiac myocyte [46], the transient changes of NADH and $[Ca^{2+}]_m$ in response to a change of workload (Fig. 9C) closely resembled the experimental results (Fig. 9A and B). Moreover, the model predicted the changes in mitochondrial ADP (ADP_m), cytoplasmic ATP (ATP_i), phosphocreatine (PCr) and average oxygen consumption (Av V_{O2}) during the protocol (Figs. 5 and 8 in Cortassa et al. [46]). After the step-increase of work, both ADP_m and Av V_{O2} abruptly increased in parallel to the initial oxidation of NADH. Since high energy phosphates were buffered by cytoplasmic PCr, the equilibrium of the reaction ATP ↔ ADP + P_i was shifted ~400-fold to the left and thus, the relative decrease of ATP after the step-increase of workload was comparably small (by 0.4% from 7.99 to 7.96 mM). This is consistent with the observation by Balaban et al. [8] who did not detect considerable changes in cellular ATP in response to up to 5-fold changes in workload in the dog heart. Due to increased ATP consumption, however, the PCr pool was continuously reduced by ~15% [46].

To test the relative contribution of ADP and $[Ca^{2+}]_m$ to the changes in respiration and NADH, distinct modifications of the model parameters were performed [46]. When halfing the rate of ATP hydrolysis by the myofibrillar ATPase (Fig. 10 B), the undershoot and overshoot of NADH were substantially reduced, while the steady-state NADH after equilibration at 2 Hz was elevated compared to control conditions (Fig. 10A). As mentioned above, this may explain why in (unstretched) cells, steady-state NADH after an increase in stimulation frequency was at a more reduced level than in (prestretched) isolated trabeculae (Fig. 9A and B; [26,101, 117]). Conversely, when reducing the maximal velocity of the mCU by 90%, mitochondrial Ca^{2+} uptake was substantially reduced (Fig. 10D), oxidation of NADH pronounced and the recovery of NADH abolished (Fig. 10C).

Taken together, both experimental results and computational modeling indicate that in response to an increase of workload, the immediate increase in respiration is mediated by ADP, while the resulting oxidation of NADH is recovered by Ca^{2+}-induced stimulation of TCA cycle enzymes. Thus, both ADP and Ca^{2+} contribute to the energetic adaptation that provides constant ATP/ADP and NADH/NAD^+ ratios in the cell.

Pathophysiological aspects

Defects in EC coupling in chronic heart failure

In chronic heart failure, contractile dysfunction is related to structural remodeling of the left ventricle and significant defects in EC coupling [13,84,94]. A major deficit in failing myocytes is the reduced Ca^{2+} content of the SR, which is related to decreased expression and activity of the SR Ca^{2+}-ATPase [84,92,146,153] and an increased Ca^{2+} leak of the RyR2 due to hyperphosphorylation [84,94,112,122]. These defects, potentially aggravated by L-type

Ca^{2+} channel dysfunction [41,71,81,86,113,131,146,184] or t-tubular derangement [32,86, 115,145,184], lead to a smaller and more dyssynchronous SR Ca^{2+} release during an AP, resulting in slower rates of increase and decay of $[Ca^{2+}]_c$, but higher diastolic $[Ca^{2+}]_c$ compared to normal cardiac myocytes [17,81,113,115,146,184]. Decreased SR Ca^{2+}-ATPase activity is partly compensated by increased expression and activity of the NCX [16,65,93,146,178,190], since pronounced forward mode I_{NCX} may maintain diastolic function [85] by removing Ca^{2+} to the extracellular space. On the other hand, this pronounced forward mode I_{NCX} may further aggravate SR Ca^{2+} depletion, since inhibition of I_{NCX} with an inhibitor peptide (XIP [118]) restored SR Ca^{2+} load in failing myocytes [91].

In heart failure, but also cardiac hypertrophy, $[Na^+]_i$ is elevated by ~3–6 mM (for review, see [156]). The physiological range of $[Na^+]_i$ in resting cardiac myocytes is ~5–15 mM and is species-dependent: While in small animals (i.e., mice and rats), $[Na^+]_i$ is between 10 and 15 mM, larger animals and humans have $[Na^+]_i$ between 5 and 10 mM [154]. $[Na^+]_i$ rises by ~3–5 mM in response to an increase of stimulation frequency [58,154,155]. In humans, $[Na^+]_i$ is 8 mM in normal resting myocytes and elevated to 12 mM in cells from patients with heart failure [155]. Similar absolute increases of $[Na^+]_i$ were observed in various animal models of cardiac failure [5,58,154] and hypertrophy [154,156].

The underlying mechanisms for elevated $[Na^+]_i$ are incompletely understood, but may involve a decrease in Na^+/K^+-ATPase activity [58,156,169,172,175,206], enhanced Na^+/H^+-exchanger (NHE) activity [2,6,40,142], or an increase in a tetrodotoxin-sensitive persistent (late) I_{Na} [58,121,203–205]. During the AP, increased $[Na^+]_i$ facilitates repolarization and pronounced cytosolic Ca^{2+}-influx via reverse-mode I_{NCX}, which partly compensates the impaired SR Ca^{2+}-release and contractility in failing myocytes [3,58,153,210,212]. In this context, the elevation of $[Na^+]_i$ in cardiac failure and hypertrophy may be regarded as a beneficial and compensatory mechanism [94]. On the other hand, cariporide, an inhibitor of the NHE, reduced $[Na^+]_i$ and improved cytosolic Ca^{2+} handling [5] and LV remodeling [6] in a rabbit heart failure model. Similarly, cariporide completely prevented the development of hypertrophy, fibrosis and heart failure in the β_1-AR overexpressing mouse [62]. These data indicate that elevated $[Na^+]_i$, besides its compensatory effects on SR Ca^{2+} load, may actually play a maladaptive role in the development of cardiac hypertrophy and failure. The precise mechanisms for such a maladaptive role, however, are currently unclear.

Are defects in EC coupling linked to energy starvation in heart failure?

Besides defects in EC coupling, the failing heart is energy-starved [99,187,211]. The total cellular levels of PCr, but also NAD and adenine nucleotides, are reduced in patients with heart failure [11,99,188]. Such changes already occur at the stage of cardiac hypertrophy [99]. In patients with heart failure, the decreased ratio of PCr/ATP predicts an adverse outcome [143]. As a more dynamic parameter of energy turnover, *in vivo* ATP flux through creatine kinase was reduced by 50% in patients with mild-to-moderate heart failure [211].

The mechanisms for the energetic deficits are manifold. As has been reviewed previously [187], mitochondria from failing hearts are characterized by more frequent membrane disruption and matrix depletion, a lower capacity for respiration with a variety of substrates, defects in complexes of the electron transport chain (ETC), and a decreased capacity for oxidative phosphorylation. Furthermore, defects in substrate metabolism such as downregulation of fatty acid oxidation and increased glycolysis and glucose oxidation may contribute to the energetic deficit [187]. Finally, mitochondria are the source for an increased production of ROS in failing hearts [97,98]. It has been proposed that increased mitochondrial ROS-production may lead to defects in mitochondrial DNA, which could contribute to reduced expression of ETC complexes in heart failure [96].

In a recent study from our lab [117], we investigated the hypothesis that an elevation of $[Na^+]_i$, as observed in heart failure, may have an adverse effect on mitochondrial energetics. Since mitochondrial Ca^{2+} efflux is governed by the mNCE with a $K_{0.5}$ for $[Na^+]_i$ in the range of ~8 mM, an increase of $[Na^+]_i$ as observed in heart failure may accelerate the rate of mitochondrial Ca^{2+} efflux and thus, decrease steady-state $[Ca^{2+}]_m$. Indeed, in isolated mitochondria, increasing extramitochondrial $[Na^+]$ decreased matrix Ca^{2+} accumulation, Ca^{2+}-stimulated activity of TCA cycle enzymes (Fig. 11), NADH production and rate of oxidative phosphorylation, while inhibition of mNCE eliminated the Na^+ sensitivity of these parameters [47,55]. Accordingly, in voltage-clamped guinea-pig cardiac myocytes, an increase of $[Na^+]_i$ from 5 to 15 mM reduced the amplitude of rapid mitochondrial Ca^{2+} transients during EC coupling by accelerating mitochondrial Ca^{2+} decay [117]. As a result, steady-state accumulation of $[Ca^{2+}]_m$ was substantially reduced (Fig. 12A and B; [117]). Physiologically, $[Na^+]_i$ is elevated in species with higher heart rates (e. g., mice or rats [154]). Furthermore, $[Na^+]_i$ generally increases at an increase of heart rate in many different species [58,154,155]. In this context, the elevation of $[Na^+]_i$ could potentially represent a physiological, protective mechanism by inhibiting mitochondrial Ca^{2+}-overload and fatal opening of the PTP [29]. On the other hand, pathophysiologically, when $[Na^+]_i$ is chronically elevated in species with normally low $[Na^+]_i$ (and slower heart rates), this may have adverse effects on mitochondrial energetics.

The transient changes of NADH in response to an abrupt increase of work (as initially characterized by Brandes and Bers (Fig. 9; [23–27]) were affected by acutely elevated $[Na^+]_i$ in a way that the initial oxidation of NADH due to ADP-induced stimulation of respiration was pronounced, whereas the (counterbalancing) recovery of NADH (related to dehydrogenation by the TCA cycle) was substantially impaired [117]. As a result, the steady-state redox potential of $NADH/NAD^+$ was oxidized at 15 compared to 5 mM $[Na^+]_i$ (Fig. 12C; [117]). Since the rate of respiration and thus, ATP production, depends on the availability of electrons to the respiratory chain in the form of NADH (Fig. 4; [45]), these results suggest that elevated $[Na^+]_i$ may critically hamper the matching process of energy supply and demand in cardiac cells.

Accordingly, in a study by Di Lisa et al. [59] on field-stimulated myocytes of the cardiomyopathic hamster, the amplitude of cytosolic Ca^{2+} transients and subsequently, mitochondrial Ca^{2+} accumulation was reduced compared to control myocytes (488 nM versus 830 nM, respectively). This was associated with reduced pyruvate dehydrogenase (PDH) activity, whose K_m for Ca^{2+} activation is in the range of ~650 nM to 1 μM (Fig. 3B; [54,56, 57,59,127,128]). Thus, both the reduced amplitude of cytosolic Ca^{2+} transients [59] and elevated $[Na^+]_i$ [117] may hamper Ca^{2+}-activation of TCA cycle enzymes in heart failure. Furthermore, glycolysis and, thus, the availability of pyruvate as a substrate for the TCA cycle was reduced in myopathic compared to control hamsters, resulting in more oxidized NADH and decreased phosphorylation potential and developed LV pressure [4]. Application of pyruvate in this model improved both energetic and hemodynamic parameters [4]. Accordingly, application of pyruvate to human heart failure patients *in vivo* increased LV systolic and diastolic function [87,88], which was related to an increase of SR Ca^{2+} load and thus, cytosolic Ca^{2+} transient amplitude *in vitro* [82,89].

Clinical implications

Taken together, these results suggest that in chronic heart failure, defects in EC coupling and glycolysis may trigger decreased supply of the respiratory chain with NADH. However, energy demand in the failing heart, despite reduced systolic Ca^{2+} transients and contractile force may be even higher than in the normal heart. First of all, due to sympathetic activation, heart rate is elevated in patients with heart failure. Furthermore, β-adrenergic activation decreases the

energetic economy of contraction in human failing myocardium [83]. An elevation of stimulation frequency increases diastolic tension (and reduces systolic force) in failing myocardium with decreased SR Ca^{2+}-ATPase expression and a lack of upregulation of the NCX [85]. Diastolic force development, however, is occurring at the same energy expenditure as systolic force generation in human failing myocardium [132]. If indeed, higher energy consumption and, thus, ATP hydrolysis occurs in failing myocardium, but with an insufficient compensatory increase of NADH production by the TCA cycle, this may explain the pronounced oxidation of the NADH-pool in failing hearts [4], which may eventually result in a mismatch between ATP supply and demand. It has been suggested that such a mismatch precedes the reduction in the total cellular levels of PCr in patients with heart failure [11,99, 188].

Besides the PCr system, which buffers high energy phosphates in the cytosol and in close spatial association with ATPases [39], direct ATP/ADP channeling also exists between mitochondria and the main sites of energy consumption, i. e., SR Ca^{2+} ATPase and myofilaments [104]. Furthermore, ATP generation from SR-associated glycolytic enzymes supports SR Ca^{2+}-ATPase activity [219]. The SR Ca^{2+}-ATPase, in fact, seems to be the most sensitive ATPase in response to a drop in the free energy released from ATP hydrolysis ($\Delta G_{\sim p}$), which may directly affect cardiac contractility [105,130,196,197,199]. This implies that decreased $\Delta G_{\sim p}$ may directly translate into defects in EC coupling and contractile function [166,196–199].Although it is difficult to determine cause and effect as the pathological conditions evolve, a vicious cycle may develop that leads to progressive cardiac dysfunction and energy starvation (Fig. 13). Interrupting this vicious cycle of defective EC coupling and energy starvation may be a novel future strategy to improve LV function, and potentially the prognosis of patients with heart failure.

In this context, approaches aimed directly at improving defective EC coupling or mitochondrial energetics (Fig. 13) without activating receptor-mediated pathways (e. g., β-adrenergic receptors) could be promising. In experimental heart failure models, transgenic inhibition or deletion of phospholamban [51,116,134] or adenoviral increase of SR Ca^{2+}-ATPase expression [52] frequently, but not always [185], improved LV function and survival. Interestingly, the increase of SR Ca^{2+}-ATPase expression was associated with an improvement of the PCr/ATP ratio in rats with heart failure after aortic banding [52], supporting the hypothesis that reconstitution of EC coupling may improve energetics. However, a specific pharmacological drug for such an intervention is currently not available.

Another concept is to inhibit forward mode I_{NCX} to increase SR Ca^{2+} load [91], however, this has not yet been tested in heart failure models *in vivo*. A traditional pharmacological approach to increase cytosolic Ca^{2+} transients is to inhibit Na^+/K^+-ATPase with digitalis, which increases $[Na^+]_i$ and thus, I_{NCX}-mediated Ca^{2+} influx. However, digitalis does not improve survival despite beneficial effects on morbidity in patients with heart failure [75]. One could speculate that adverse energetic effects by the concomitant increase of $[Na^+]_i$ (and consequent effects on mitochondrial Ca^{2+} handling) could explain this lack of prognostic benefit [6,117]. Furthermore, besides inhibiting Na^+/K^+-ATPase, digitalis may have other yet unknown effects improving contractility [207,218].

Thus, in the light of a potential maladaptive role of elevated $[Na^+]_i$ in heart failure, it may be a promising approach to reduce cellular Na^+-influx. This could be achieved by inhibiting I_{NHE} or late I_{Na}. Both approaches were cardioprotective in experimental models of ischemia/ reperfusion, since in this situation, an excessive increase of $[Na^+]_i$ contributes to progressive cytosolic and mitochondrial Ca^{2+}-overload and thus, the induction of apoptosis through activation of the mitochondrial PTP [78,135,168,189]. Also in animal models of heart failure, both the inhibition of I_{NHE} by cariporide and of late I_{Na} by ranolazine reduced $[Na^+]_i$ and

improved EC coupling and LV remodeling [6,34,38,62,163,202]. In conditions of cardiac ischemia/reperfusion, inhibition of I_{NHE} preserved mitochondrial energetics (i.e., ATP and PCr content) [111,162]. However, these effects were not related to an improvement of EC coupling, but rather to a delay of mitochondrial matrix acidification by a mechanism unrelated to the sarcolemmal NHE [162]. Furthermore, beneficial effects of ranolazine on mitochondrial energetics have so far been related to its ability to decrease fatty-acid oxidation, promote glucose oxidation, and by increasing pyruvate dehydrogenase complex activity [1,125,192] rather than by improving EC coupling. Thus, at this point, it is unknown whether reducing $[Na^+]_i$ per se improves mitochondrial energetics, especially in heart failure.

A novel target to improve mitochondrial energetics and cardiac function in heart failure or ischemia/reperfusion could be to inhibit the mNCE. While elevated $[Na^+]_i$ reduced steady-state $[Ca^{2+}]_m$, TCA cycle activity and rate of oxidative phosphorylation, inhibiting the mNCE with CGP-37157 improved mitochondrial Ca^{2+}-accumulation and energetics in isolated mitochondria and cardiac myocytes [47,114,117]. Furthermore, during ischemia and reperfusion with cytosolic Ca^{2+} overload and a collapse of $\Delta\psi_m$, the mNCE in *reverse* mode has been shown to contribute to mitochondrial Ca^{2+} overload [180], which eventually may lead to PTP opening and cell death [29]. In this setting, CGP-37157 inhibited mitochondrial Ca^{2+} overload [180]. Thus, inhibiting the mNCE may improve energetics and potentially protect from apoptosis in various pathologic situations. However, data on the effects of mNCE-inhibition on cardiac energetics *in vivo* are presently not available. Furthermore, considering that the physiological increase of $[Na^+]_i$ during an increase of heart rate [58,154,155] could potentially prevent mitochondrial Ca^{2+} overload (as discussed in the previous chapter), it remains unclear whether mNCE-inhibition may have adverse effects on energetics under physiological conditions. Clearly, more *in vitro* and *in vivo* research is needed to further evaluate the mNCE as a therapeutic target.

In conclusion, the processes of EC coupling and mitochondrial energetics are highly interrelated, and defects in EC coupling may directly translate into defects in mitochondrial energetics in pathological situations. The understanding of the relation between EC coupling and energetics may help to develop new strategies to improve LV function and potentially survival in patients with chronic heart failure.

Acknowledgments

C. Maack is supported by the Deutsche Forschungsgemeinschaft (Emmy Noether-Programm).B.O'Rourke is supported by the NIH (R37HL54598 and P01 HL081427).

References

1. Abozguia K, Clarke K, Lee L, Frenneaux M. Modification of myocardial substrate use as a therapy for heart failure. Nat Clin Pract Cardiovasc Med 2006;3:490–498. [PubMed: 16932766]
2. Aker S, Snabaitis AK, Konietzka I, Van De Sand A, Bongler K, Avkiran M, Heusch G, Schulz R. Inhibition of the Na^+/H^+ exchanger attenuates the deterioration of ventricular function during pacing-induced heart failure in rabbits. Cardiovasc Res 2004;63:273–282. [PubMed: 15249185]
3. Armoundas AA, Hobai IA, Tomaselli GF, Winslow RL, O'Rourke B. Role of sodium-calcium exchanger in modulating the action potential of ventricular myocytes from normal and failing hearts. Circ Res 2003;93:46–53. [PubMed: 12805237]
4. Auffermann W, Wu ST, Parmley WW, Wikman-Coffelt J. Glycolysis in heart failure: a 31P-NMR and surface fluorometry study. Basic Res Cardiol 1990;85:342–357. [PubMed: 2241766]
5. Baartscheer A, Schumacher CA, van Borren MM, Belterman CN, Coronel R, Fiolet JW. Increased Na^+/H^+-exchange activity is the cause of increased $[Na^+]_i$ and underlies disturbed calcium handling in the rabbit pressure and volume overload heart failure model. Cardiovasc Res 2003;57:1015–1024. [PubMed: 12650879]

6. Baartscheer A, Schumacher CA, van Borren MM, Belterman CN, Coronel R, Opthof T, Fiolet JW. Chronic inhibition of Na^+/H^+-exchanger attenuates cardiac hypertrophy and prevents cellular remodeling in heart failure. Cardiovasc Res 2005;65:83–92. [PubMed: 15621036]
7. Balaban RS. Cardiac energy metabolism homeostasis: role of cytosolic calcium. J Mol Cell Cardiol 2002;34:1259–1271. [PubMed: 12392982]
8. Balaban RS, Kantor HL, Katz LA, Briggs RW. Relation between work and phosphate metabolite in the in vivo paced mammalian heart. Science 1986;232:1121–1123. [PubMed: 3704638]
9. Bassani RA, Bassani JW, Bers DM. Mitochondrial and sarcolemmal Ca^{2+} transport reduce $[Ca^{2+}]_i$ during caffeine contractures in rabbit cardiac myocytes. J Physiol 1992;453:591–608. [PubMed: 1464847]
10. Baysal K, Jung DW, Gunter KK, Gunter TE, Brierley GP. $Na(^+)$-dependent Ca^{2+} efflux mechanism of heart mitochondria is not a passive $Ca^{2+}/2Na^+$ exchanger. Am J Physiol 1994;266:C800–C808. [PubMed: 8166244]
11. Beer M, Seyfarth T, Sandstede J, Landschutz W, Lipke C, Kostler H, von Kienlin M, Harre K, Hahn D, Neubauer S. Absolute concentrations of high-energy phosphate metabolites in normal, hypertrophied, and failing human myocardium measured noninvasively with (31)P-SLOOP magnetic resonance spectroscopy. J Am Coll Cardiol 2002;40:1267–1274. [PubMed: 12383574]
12. Bell CJ, Bright NA, Rutter GA, Griffiths EJ. ATP regulation in adult rat cardiomyocytes: Time resolved decoding of rapid mitochondrial calcium spiking imaged with targeted photoproteins. J Biol Chem 2006;281:28058–28067. [PubMed: 16882672]
13. Bers DM. Altered Cardiac Myocyte Ca Regulation In Heart Failure. Physiology (Bethesda) 2006;21:380–387. [PubMed: 17119150]
14. Bers DM. Cardiac excitation-contraction coupling. Nature 2002;415:198–205. [PubMed: 11805843]
15. Bers, DM. Dordrecht, The Netherlands: Kluwer Academic Publisher; 2001. Excitation-contraction coupling and cardiac contractile force.
16. Bers DM, Pogwizd SM, Schlotthauer K. Upregulated Na/Ca exchange is involved in both contractile dysfunction and arrhythmogenesis in heart failure. Basic Res Cardiol 2002;97(Suppl 1):I36–I42. [PubMed: 12479232]
17. Beuckelmann DJ, Näbauer M, Erdmann E. Intracellular calcium handling in isolated ventricular myocytes from patients with terminal heart failure. Circulation 1992;85:1046–1055. [PubMed: 1311223]
18. Beutner G, Sharma VK, Giovannucci DR, Yule DI, Sheu SS. Identification of a ryanodine receptor in rat heart mitochondria. J Biol Chem 2001;276:21482–21488. [PubMed: 11297554]
19. Beutner G, Sharma VK, Lin L, Ryu SY, Dirksen RT, Sheu SS. Type 1 ryanodine receptor in cardiac mitochondria: transducer of excitation-metabolism coupling. Biochim Biophys Acta 2005;1717:1–10. [PubMed: 16246297]
20. Bootman MD, Higazi DR, Coombes S, Roderick HL. Calcium signalling during excitation-contraction coupling in mammalian atrial myocytes. J Cell Sci 2006;119:3915–3925. [PubMed: 16988026]
21. Bose S, French S, Evans FJ, Joubert F, Balaban RS. Metabolic network control of oxidative phosphorylation: multiple roles of inorganic phosphate. J Biol Chem 2003;278:39155–39165. [PubMed: 12871940]
22. Bowditch HP. Über die Eigenthümlichkeiten der Reizbarkeit, welche die Muskelfasern des Herzens zeigen. Ber Sächs Akad Wiss 1871;23:652–689.
23. Brandes R, Bers DM. Analysis of the mechanisms of mitochondrial NADH regulation in cardiac trabeculae. Biophys J 1999;77:1666–1682. [PubMed: 10465777]
24. Brandes R, Bers DM. Increased work in cardiac trabeculae causes decreased mitochondrial NADH fluorescence followed by slow recovery. Biophys J 1996;71:1024–1035. [PubMed: 8842239]
25. Brandes R, Bers DM. Intracellular Ca^{2+} increases the mitochondrial NADH concentration during elevated work in intact cardiac muscle. Circ Res 1997;80:82–87. [PubMed: 8978326]
26. Brandes R, Bers DM. Simultaneous measurements of mitochondrial NADH and $Ca(^{2+})$ during increased work in intact rat heart trabeculae. Biophys J 2002;83:587–604. [PubMed: 12124250]

27. Brandes R, Maier LS, Bers DM. Regulation of mitochondrial [NADH] by cytosolic [Ca^{2+}] and work in trabeculae from hypertrophic and normal rat hearts. Circ Res 1998;82:1189–1198. [PubMed: 9633918]
28. Brodde OE, Michel MC. Adrenergic and muscarinic receptors in the human heart. Pharmacol Rev 1999;51:651–690. [PubMed: 10581327]
29. Brookes PS, Yoon Y, Robotham JL, Anders MW, Sheu SS. Calcium, ATP, and ROS: a mitochondrial love-hate triangle. Am J Physiol Cell Physiol 2004;287:C817–C833. [PubMed: 15355853]
30. Buntinas L, Gunter KK, Sparagna GC, Gunter TE. The rapid mode of calcium uptake into heart mitochondria (RaM): comparison to RaM in liver mitochondria. Biochim Biophys Acta 2001;1504:248–261. [PubMed: 11245789]
31. Cannell MB, Cheng H, Lederer WJ. Spatial non-uniformities in $[Ca^{2+}]_i$ during excitation-contraction coupling in cardiac myocytes. Biophys J 1994;67:1942–1956. [PubMed: 7858131]
32. Cannell MB, Crossman DJ, Soeller C. Effect of changes in action potential spike configuration, junctional sarcoplasmic reticulum micro-architecture and altered t-tubule structure in human heart failure. J Muscle Res Cell Motil 2006;27:297–306. [PubMed: 16897575]
33. Chacon E, Ohata H, Harper IS, Trollinger DR, Herman B, Lemasters JJ. Mitochondrial free calcium transients during excitation-contraction coupling in rabbit cardiac myocytes. FEBS Lett 1996;382:31–36. [PubMed: 8612759]
34. Chaitman BR. Ranolazine for the treatment of chronic angina and potential use in other cardiovascular conditions. Circulation 2006;113:2462–2472. [PubMed: 16717165]
35. Chamberlain BK, Volpe P, Fleischer S. Inhibition of calcium-induced calcium release from purified cardiac sarcoplasmic reticulum vesicles. J Biol Chem 1984;259:7547–7553. [PubMed: 6736019]
36. Chance B. The Energy-Linked Reaction of Calcium with Mitochondria. J Biol Chem 1965;240:2729–2748. [PubMed: 14304892]
37. Chance B, Williams GR. A method for the localization of sites for oxidative phosphorylation. Nature 1955;176:250–254. [PubMed: 13244669]
38. Chandler MP, Stanley WC, Morita H, Suzuki G, Roth BA, Blackburn B, Wolff A, Sabbah HN. Short-term treatment with ranolazine improves mechanical efficiency in dogs with chronic heart failure. Circ Res 2002;91:278–280. [PubMed: 12193459]
39. Chazov EI, Smirnov VN, Saks VA, Rosenshtraukh LV, Lipina NV, Levitsky DO. Energy metabolism and ion fluxes across cardiac membranes. Adv Myocardiol 1980;1:139–153. [PubMed: 6248931]
40. Chen L, Chen CX, Gan XT, Beier N, Scholz W, Karmazyn M. Inhibition and reversal of myocardial infarction-induced hypertrophy and heart failure by NHE-1 inhibition. Am J Physiol Heart Circ Physiol 2004;286:H381–H387. [PubMed: 14684366]
41. Chen X, Piacentino V 3rd, Furukawa S, Goldman B, Margulies KB, Houser SR. L-type Ca^{2+} channel density and regulation are altered in failing human ventricular myocytes and recover after support with mechanical assist devices. Circ Res 2002;91:517–524. [PubMed: 12242270]
42. Cheng H, Lederer WJ, Cannell MB. Calcium sparks: elementary events underlying excitation-contraction coupling in heart muscle. Science 1993;262:740–744. [PubMed: 8235594]
43. Chen-Izu Y, McCulle SL, Ward CW, Soeller C, Allen BM, Rabang C, Cannell MB, Balke CW, Izu LT. Three-dimensional distribution of ryanodine receptor clusters in cardiac myocytes. Biophys J 2006;91:1–13. [PubMed: 16603500]
44. Collins TJ, Lipp P, Berridge MJ, Bootman MD. Mitochondrial Ca($^{2+}$) uptake depends on the spatial and temporal profile of cytosolic Ca($^{2+}$) signals. J Biol Chem 2001;276:26411–26420. [PubMed: 11333261]
45. Cortassa S, Aon MA, Marban E, Winslow RL, O'Rourke B. An integrated model of cardiac mitochondrial energy metabolism and calcium dynamics. Biophys J 2003;84:2734–2755. [PubMed: 12668482]
46. Cortassa S, Aon MA, O'Rourke B, Jacques R, Tseng HJ, Marban E, Winslow RL. A computational model integrating electrophysiology, contraction, and mitochondrial bioenergetics in the ventricular myocyte. Biophys J 2006;91:1564–1589. [PubMed: 16679365]
47. Cox DA, Matlib MA. A role for the mitochondrial Na($^{+}$)-Ca^{2+} exchanger in the regulation of oxidative phosphorylation in isolated heart mitochondria. J Biol Chem 1993;268:938–947. [PubMed: 8419373]

48. Crompton M. The sodium ion/calcium ion cycle of cardiac mitochondria. Biochem Soc Trans 1980;8:261–262. [PubMed: 6249667]
49. Crompton M, Kunzi M, Carafoli E. The calcium-induced and sodium-induced effluxes of calcium from heart mitochondria. Evidence for a sodium-calcium carrier. Eur J Biochem 1977;79:549–558. [PubMed: 923566]
50. Davidson SM, Duchen MR. Calcium microdomains and oxidative stress. Cell Calcium 2006;40:561–574. [PubMed: 17049598]
51. del Monte F, Harding SE, Dec GW, Gwathmey JK, Hajjar RJ. Targeting phospholamban by gene transfer in human heart failure. Circulation 2002;105:904–907. [PubMed: 11864915]
52. del Monte F, Williams E, Lebeche D, Schmidt U, Rosenzweig A, Gwathmey JK, Lewandowski ED, Hajjar RJ. Improvement in survival and cardiac metabolism after gene transfer of sarcoplasmic reticulum Ca($^{2+}$)-ATPase in a rat model of heart failure. Circulation 2001;104:1424–1429. [PubMed: 11560860]
53. Denton RM, McCormack JG. Ca^{2+} as a second messenger within mitochondria of the heart and other tissues. Annual Review of Physiology 1990;52:451–466.
54. Denton RM, McCormack JG. Ca^{2+} transport by mammalian mitochondria and its role in hormone action. Am J Physiol 1985;249:E543–E554. [PubMed: 2417490]
55. Denton RM, McCormack JG, Edgell NJ. Role of calcium ions in the regulation of intramitochondrial metabolism. Effects of Na^{+} , Mg^{2+} and ruthenium red on the Ca^{2+} -stimulated oxidation of oxoglutarate and on pyruvate dehydrogenase activity in intact rat heart mitochondria. Biochem J 1980;190:107–117. [PubMed: 6160850]
56. Denton RM, Randle PJ, Martin BR. Stimulation by calcium ions of pyruvate dehydrogenase phosphate phosphatase. Biochem J 1972;128:161–163. [PubMed: 4343661]
57. Denton RM, Richards DA, Chin JG. Calcium ions and the regulation of NAD^{+}-linked isocitrate dehydrogenase from the mitochondria of rat heart and other tissues. Biochem J 1978;176:899–906. [PubMed: 218557]
58. Despa S, Islam MA, Weber CR, Pogwizd SM, Bers DM. Intracellular Na($^{+}$) concentration is elevated in heart failure but Na/K pump function is unchanged. Circulation 2002;105:2543–2548. [PubMed: 12034663]
59. Di Lisa F, Fan CZ, Gambassi G, Hogue BA, Kudryashova I, Hansford RG. Altered pyruvate dehydrogenase control and mitochondrial free Ca^{2+} in hearts of cardiomyopathic hamsters. Am J Physiol 1993;264:H2188–H2197. [PubMed: 8322950]
60. Di Lisa F, Gambassi G, Spurgeon H, Hansford RG. Intramitochondrial free calcium in cardiac myocytes in relation to dehydrogenase activation. Cardiovasc Res 1993;27:1840–1844. [PubMed: 8275533]
61. Duchen MR, Leyssens A, Crompton M. Transient mitochondrial depolarizations reflect focal sarcoplasmic reticular calcium release in single rat cardiomyocytes. J Cell Biol 1998;142:975–988. [PubMed: 9722610]
62. Engelhardt S, Hein L, Keller U, Klambt K, Lohse MJ. Inhibition of Na($^{+}$)-H($^{+}$) exchange prevents hypertrophy, fibrosis, and heart failure in beta(1)-adrenergic receptor transgenic mice. Circ Res 2002;90:814–819. [PubMed: 11964375]
63. Fabiato A. Simulated calcium current can both cause calcium loading in and trigger calcium release from the sarcoplasmic reticulum of a skinned canine cardiac Purkinje cell. J Gen Physiol 1985;85:291–320. [PubMed: 2580044]
64. Fabiato A. Time and calcium dependence of activation and inactivation of calcium-induced release of calcium from the sarcoplasmic reticulum of a skinned canine cardiac Purkinje cell. J Gen Physiol 1985;85:247–289. [PubMed: 2580043]
65. Flesch M, Schwinger RH, Schiffer F, Frank K, Sudkamp M, Kuhn-Regnier F, Arnold G, Bohm M. Evidence for functional relevance of an enhanced expression of the Na($^{+}$)-Ca^{2+} exchanger in failing human myocardium. Circulation 1996;94:992–1002. [PubMed: 8790037]
66. Frank O. Zur Dynamik des Herzmuskels. Z Biologie 1885;32:370–447.
67. Fry CH, Powell T, Twist VW, Ward JP. Net calcium exchange in adult rat ventricular myocytes: an assessment of mitochondrial calcium accumulating capacity. Proc R Soc Lond B Biol Sci 1984;223:223–238. [PubMed: 6151661]

68. Gallitelli MF, Schultz M, Isenberg G, Rudolf F. Twitch-potentiation increases calcium in peripheral more than in central mitochondria of guinea-pig ventricular myocytes. J Physiol 1999;518(Pt 2):433–447. [PubMed: 10381590]
69. Gavin CE, Gunter KK, Gunter TE. Manganese and calcium efflux kinetics in brain mitochondria. Relevance to manganese toxicity. Biochem J 1990;266:329–334. [PubMed: 2317189]
70. Gavin CE, Gunter KK, Gunter TE. Mn^{2+} sequestration by mitochondria and inhibition of oxidative phosphorylation. Toxicol Appl Pharmacol 1992;115:1–5. [PubMed: 1631887]
71. Gomez AM, Valdivia HH, Cheng H, Lederer MR, Santana LF, Cannell MB, McCune SA, Altschuld RA, Lederer WJ. Defective excitation-contraction coupling in experimental cardiac hypertrophy and heart failure. Science 1997;276:800–806. [PubMed: 9115206]
72. Griffiths EJ. Species dependence of mitochondrial calcium transients during excitation-contraction coupling in isolated cardiomyocytes. Biochem Biophys Res Commun 1999;263:554–559. [PubMed: 10491330]
73. Griffiths EJ, Stern MD, Silverman HS. Measurement of mitochondrial calcium in single living cardiomyocytes by selective removal of cytosolic indo 1. Am J Physiol 1997;273:C37–C44. [PubMed: 9252440]
74. Griffiths EJ, Wei SK, Haigney MC, Ocampo CJ, Stern MD, Silverman HS. Inhibition of mitochondrial calcium efflux by clonazepam in intact single rat cardiomyocytes and effects on NADH production. Cell Calcium 1997;21:321–329. [PubMed: 9160168]
75. Group TDI. The effect of digoxin on mortality and morbidity in patients with heart failure. N Engl J Med 1997;336:525–533. [PubMed: 9036306]
76. Gunter TE, Gunter KK, Sheu SS, Gavin CE. Mitochondrial calcium transport: physiological and pathological relevance. Am J Physiol 1994;267:C313–C339. [PubMed: 8074170]
77. Gunter TE, Pfeiffer DR. Mechanisms by which mitochondria transport calcium. Am J Physiol 1990;258:C755–C786. [PubMed: 2185657]
78. Hale SL, Leeka JA, Kloner RA. Improved left ventricular function and reduced necrosis after myocardial ischemia/reperfusion in rabbits treated with ranolazine, an inhibitor of the late sodium channel. J Pharmacol Exp Ther 2006;318:418–423. [PubMed: 16617168]
79. Hansford RG. Relation between mitochondrial calcium transport and control of energy metabolism. Rev Physiol Biochem Pharmacol 1985;102:1–72. [PubMed: 2863864]
80. Harris DA, Das AM. Control of mitochondrial ATP synthesis in the heart. Biochem J 1991;280(Pt 3):561–573. [PubMed: 1837214]
81. Harris DM, Mills GD, Chen X, Kubo H, Berretta RM, Votaw VS, Santana LF, Houser SR. Alterations in early action potential repolarization causes localized failure of sarcoplasmic reticulum Ca^{2+} release. Circ Res 2005;96:543–550. [PubMed: 15705962]
82. Hasenfuss G, Maier LS, Hermann HP, Luers C, Hunlich M, Zeitz O, Janssen PM, Pieske B. Influence of pyruvate on contractile performance and $Ca(^{2+})$ cycling in isolated failing human myocardium. Circulation 2002;105:194–199. [PubMed: 11790700]
83. Hasenfuss G, Mulieri LA, Allen PD, Just H, Alpert NR. Influence of isoproterenol and ouabain on excitation-contraction coupling, cross-bridge function, and energetics in failing human myocardium. Circulation 1996;94:3155–3160. [PubMed: 8989123]
84. Hasenfuss G, Pieske B. Calcium cycling in congestive heart failure. J Mol Cell Cardiol 2002;34:951–969. [PubMed: 12234765]
85. Hasenfuss G, Schillinger W, Lehnart SE, Preuss M, Pieske B, Maier LS, Prestle J, Minami K, Just H. Relationship between Na^{+}-Ca^{2+}-exchanger protein levels and diastolic function of failing human myocardium. Circulation 1999;99:641–648. [PubMed: 9950661]
86. He J, Conklin MW, Foell JD, Wolff MR, Haworth RA, Coronado R, Kamp TJ. Reduction in density of transverse tubules and L-type $Ca(^{2+})$ channels in canine tachycardia-induced heart failure. Cardiovasc Res 2001;49:298–307. [PubMed: 11164840]
87. Hermann HP, Arp J, Pieske B, Kogler H, Baron S, Janssen PM, Hasenfuss G. Improved systolic and diastolic myocardial function with intracoronary pyruvate in patients with congestive heart failure. Eur J Heart Fail 2004;6:213–218. [PubMed: 14984729]

88. Hermann HP, Pieske B, Schwarzmuller E, Keul J, Just H, Hasenfuss G. Haemodynamic effects of intracoronary pyruvate in patients with congestive heart failure: an open study. Lancet 1999;353:1321–1323. [PubMed: 10218531]

89. Hermann HP, Zeitz O, Lehnart SE, Keweloh B, Datz N, Hasenfuss G, Janssen PM. Potentiation of beta-adrenergic inotropic response by pyruvate in failing human myocardium. Cardiovasc Res 2002;53:116–123. [PubMed: 11744019]

90. Hille, B. Ion Channels of Excitable Membranes. Sunderland, Massachusetts: Sinauer Associates; 2001.

91. Hobai IA, Maack C, O'Rourke B. Partial inhibition of sodium/calcium exchange restores cellular calcium handling in canine heart failure. Circ Res 2004;95:292–299. [PubMed: 15217911]

92. Hobai IA, O'Rourke B. Decreased sarcoplasmic reticulum calcium content is responsible for defective excitation-contraction coupling in canine heart failure. Circulation 2001;103:1577–1584. [PubMed: 11257088]

93. Hobai IA, O'Rourke B. Enhanced $Ca(^{2+})$-activated $Na(^{+})$-$Ca(^{2+})$ exchange activity in canine pacing-induced heart failure. Circ Res 2000;87:690–698. [PubMed: 11029405]

94. Houser SR, Margulies KB. Is depressed myocyte contractility centrally involved in heart failure? Circ Res 2003;92:350–358. [PubMed: 12623873]

95. Huser J, Blatter LA, Sheu SS. Mitochondrial calcium in heart cells: beat-to-beat oscillations or slow integration of cytosolic transients? J Bioenerg Biomembr 2000;32:27–33. [PubMed: 11768759]

96. Ide T, Tsutsui H, Hayashidani S, Kang D, Suematsu N, Nakamura K, Utsumi H, Hamasaki N, Takeshita A. Mitochondrial DNA damage and dysfunction associated with oxidative stress in failing hearts after myocardial infarction. Circ Res 2001;88:529–535. [PubMed: 11249877]

97. Ide T, Tsutsui H, Kinugawa S, Suematsu N, Hayashidani S, Ichikawa K, Utsumi H, Machida Y, Egashira K, Takeshita A. Direct evidence for increased hydroxyl radicals originating from superoxide in the failing myocardium. Circ Res 2000;86:152–157. [PubMed: 10666410]

98. Ide T, Tsutsui H, Kinugawa S, Utsumi H, Kang D, Hattori N, Uchida K, Arimura K, Egashira K, Takeshita A. Mitochondrial electron transport complex I is a potential source of oxygen free radicals in the failing myocardium. Circ Res 1999;85:357–363. [PubMed: 10455064]

99. Ingwall JS, Weiss RG. Is the failing heart energy starved? On using chemical energy to support cardiac function. Circ Res 2004;95:135–145. [PubMed: 15271865]

100. Isenberg G, Han S, Schiefer A, Wendt-Gallitelli MF. Changes in mitochondrial calcium concentration during the cardiac contraction cycle. Cardiovasc Res 1993;27:1800–1809. [PubMed: 8275527]

101. Jo H, Noma A, Matsuoka S. Calcium-mediated coupling between mitochondrial substrate dehydrogenation and cardiac workload in single guinea-pig ventricular myocytes. J Mol Cell Cardiol 2006;40:394–404. [PubMed: 16480740]

102. Jones PP, Bazzazi H, Kargacin GJ, Colyer J. Inhibition of cAMP-dependent protein kinase under conditions occurring in the cardiac dyad during a Ca^{2+} transient. Biophys J 2006;91:433–443. [PubMed: 16632511]

103. Jung DW, Baysal K, Brierley GP. The sodium-calcium antiport of heart mitochondria is not electroneutral. J Biol Chem 1995;270:672–678. [PubMed: 7822294]

104. Kaasik A, Veksler V, Boehm E, Novotova M, Minajeva A, Ventura-Clapier R. Energetic crosstalk between organelles: architectural integration of energy production and utilization. Circ Res 2001;89:153–159. [PubMed: 11463722]

105. Kammermeier H. High energy phosphate of the myocardium: concentration versus free energy change. Basic Res Cardiol 1987;82(Suppl 2):31–36. [PubMed: 2959262]

106. Katz LA, Koretsky AP, Balaban RS. Activation of dehydrogenase activity and cardiac respiration: a 31P-NMR study. Am J Physiol 1988;255:H185–H188. [PubMed: 2456023]

107. Katz LA, Koretsky AP, Balaban RS. Respiratory control in the glucose perfused heart. A 31P NMR and NADH fluorescence study. FEBS Lett 1987;221:270–276. [PubMed: 3622766]

108. Katz LA, Swain JA, Portman MA, Balaban RS. Relation between phosphate metabolites and oxygen consumption of heart in vivo. Am J Physiol 1989;256:H265–H274. [PubMed: 2912189]

109. Kirichok Y, Krapivinsky G, Clapham DE. The mitochondrial calcium uniporter is a highly selective ion channel. Nature 2004;427:360–364. [PubMed: 14737170]

110. Kockskamper J, Sheehan KA, Bare DJ, Lipsius SL, Mignery GA, Blatter LA. Activation and propagation of Ca($^{2+}$) release during excitation-contraction coupling in atrial myocytes. Biophys J 2001;81:2590–2605. [PubMed: 11606273]
111. Lee BH, Seo HW, Yi KY, Lee S, Yoo SE. Effects of KR-32570, a new Na^+/H^+ exchanger inhibitor, on functional and metabolic impairments produced by global ischemia and reperfusion in the perfused rat heart. Eur J Pharmacol 2005;511:175–182. [PubMed: 15792786]
112. Lehnart SE, Wehrens XH, Marks AR. Defective ryanodine receptor interdomain interactions may contribute to intracellular Ca^{2+} leak: a novel therapeutic target in heart failure. Circulation 2005;111:3342–3346. [PubMed: 15983258]
113. Litwin SE, Zhang D, Bridge JH. Dyssynchronous Ca($^{2+}$) sparks in myocytes from infarcted hearts. Circ Res 2000;87:1040–1047. [PubMed: 11090550]
114. Liu T, O'Rourke B. Enhancing Mitochondrial Ca^{2+} Uptake Restores Energy Supply and Demand Matching at High Cytosolic Na^+ in Cardiomyocytes. Biophys J 2007;922198-Pos/B2414 (Abstract)
115. Louch WE, Bito V, Heinzel FR, Macianskiene R, Vanhaecke J, Flameng W, Mubagwa K, Sipido KR. Reduced synchrony of Ca^{2+} release with loss of T-tubules – a comparison to Ca^{2+} release in human failing cardiomyocytes. Cardiovasc Res 2004;62:63–73. [PubMed: 15023553]
116. Luo W, Grupp IL, Harrer J, Ponniah S, Grupp G, Duffy JJ, Doetschman T, Kranias EG. Targeted ablation of the phospholamban gene is associated with markedly enhanced myocardial contractility and loss of beta-agonist stimulation. Circ Res 1994;75:401–409. [PubMed: 8062415]
117. Maack C, Cortassa S, Aon MA, Ganesan AN, Liu T, O'Rourke B. Elevated cytosolic Na^+ decreases mitochondrial Ca^{2+} uptake during excitation-contraction coupling and impairs energetic adaptation in cardiac myocytes. Circ Res 2006;99:172–182. [PubMed: 16778127]
118. Maack C, Ganesan A, Sidor A, O'Rourke B. Cardiac sodium-calcium exchanger is regulated by allosteric calcium and exchanger inhibitory peptide at distinct sites. Circ Res 2005;96:91–99. [PubMed: 15550690]
119. Mackenzie L, Roderick HL, Berridge MJ, Conway SJ, Bootman MD. The spatial pattern of atrial cardiomyocyte calcium signalling modulates contraction. J Cell Sci 2004;117:6327–6337. [PubMed: 15561771]
120. Maier LS, Bers DM. Role of Ca^{2+}/calmodulin-dependent protein kinase (CaMK) in excitation-contraction coupling in the heart. Cardiovasc Res 2007;73:631–640. [PubMed: 17157285]
121. Maltsev VA, Sabbah HN, Undrovinas AI. Late sodium current is a novel target for amiodarone: studies in failing human myocardium. J Mol Cell Cardiol 2001;33:923–932. [PubMed: 11343415]
122. Marx SO, Reiken S, Hisamatsu Y, Jayaraman T, Burkhoff D, Rosemblit N, Marks AR. PKA phosphorylation dissociates FKBP12.6 from the calcium release channel (ryanodine receptor): defective regulation in failing hearts. Cell 2000;101:365–376. [PubMed: 10830164]
123. Masumiya H, Tsujikawa H, Hino N, Ochi R. Modulation of manganese currents by 1:4-dihydropyridines, isoproterenol and forskolin in rabbit ventricular cells. Pflugers Arch 2003;446:695–701. [PubMed: 12827360]
124. Matlib MA, Zhou Z, Knight S, Ahmed S, Choi KM, Krause-Bauer J, Phillips R, Altschuld R, Katsube Y, Sperelakis N, Bers DM. Oxygen-bridged di-nuclear ruthenium amine complex specifically inhibits Ca^{2+} uptake into mitochondria in vitro and in situ in single cardiac myocytes. J Biol Chem 1998;273:10223–10231. [PubMed: 9553073]
125. McCormack JG, Barr RL, Wolff AA, Lopaschuk GD. Ranolazine stimulates glucose oxidation in normoxic, ischemic, and reperfused ischemic rat hearts. Circulation 1996;93:135–142. [PubMed: 8616920]
126. McCormack JG, Browne HM, Dawes NJ. Studies on mitochondrial Ca^{2+}-transport and matrix Ca^{2+} using fura-2-loaded rat heart mitochondria. Biochim Biophys Acta 1989;973:420–427. [PubMed: 2923871]
127. McCormack JG, Denton RM. The effects of calcium ions and adenine nucleotides on the activity of pig heart 2-oxoglutarate dehydrogenase complex. Biochem J 1979;180:533–544. [PubMed: 39549]
128. McCormack JG, Denton RM. Role of Ca^{2+} ions in the regulation of intramitochondrial metabolism in rat heart. Evidence from studies with isolated mitochondria that adrenaline activates the pyruvate

dehydrogenase and 2-oxoglutarate dehydrogenase complexes by increasing the intramitochondrial concentration of Ca^{2+} Biochem J 1984;218:235–247. [PubMed: 6424656]

129. McCormack JG, Halestrap AP, Denton RM. Role of calcium ions in regulation of mammalian intramitochondrial metabolism. Physiol Rev 1990;70:391–425. [PubMed: 2157230]
130. McCutcheon LJ, Cory CR, Nowack L, Shen H, Mirsalami M, Lahucky R, Kovac L, O'Grady M, Horne R, O'Brien PJ. Respiratory chain defect of myocardial mitochondria in idiopathic dilated cardiomyopathy of Doberman pinscher dogs. Can J Physiol Pharmacol 1992;70:1529–1533. [PubMed: 1338376]
131. Mewes T, Ravens U. L-type calcium currents of human myocytes from ventricle of non-failing and failing hearts and from atrium. J Mol Cell Cardiol 1994;26:1307–1320. [PubMed: 7869391]
132. Meyer M, Keweloh B, Guth K, Holmes JW, Pieske B, Lehnart SE, Just H, Hasenfuss G. Frequency-dependence of myocardial energetics in failing human myocardium as quantified by a new method for the measurement of oxygen consumption in muscle strip preparations. J Mol Cell Cardiol 1998;30:1459–1470. [PubMed: 9737933]
133. Michailova A, McCulloch A. Model study of ATP and ADP buffering, transport of Ca($^{2+}$) and Mg ($^{2+}$), and regulation of ion pumps in ventricular myocyte. Biophys J 2001;81:614–629. [PubMed: 11463611]
134. Minamisawa S, Hoshijima M, Chu G, Ward CA, Frank K, Gu Y, Martone ME, Wang Y, Ross J Jr, Kranias EG, Giles WR, Chien KR. Chronic phospholamban-sarcoplasmic reticulum calcium ATPase interaction is the critical calcium cycling defect in dilated cardiomyopathy. Cell 1999;99:313–322. [PubMed: 10555147]
135. Miura T, Ogawa T, Suzuki K, Goto M, Shimamoto K. Infarct size limitation by a new Na($^{+}$)-H^{+} exchange inhibitor, Hoe 642: difference from preconditioning in the role of protein kinase C. J Am Coll Cardiol 1997;29:693–701. [PubMed: 9060913]
136. Miyata H, Lakatta EG, Stern MD, Silverman HS. Relation of mitochondrial and cytosolic free calcium to cardiac myocyte recovery after exposure to anoxia. Circ Res 1992;71:605–613. [PubMed: 1499108]
137. Miyata H, Silverman HS, Sollott SJ, Lakatta EG, Stern MD, Hansford RG. Measurement of mitochondrial free Ca^{2+} concentration in living single rat cardiac myocytes. Am J Physiol 1991;261:H1123–H1134. [PubMed: 1928394]
138. Moore CL. Specific inhibition of mitochondrial Ca^{++} transport by ruthenium red. Biochem Biophys Res Commun 1971;42:298–305. [PubMed: 4250976]
139. Mootha VK, Arai AE, Balaban RS. Maximum oxidative phosphorylation capacity of the mammalian heart. Am J Physiol 1997;272:H769–H775. [PubMed: 9124437]
140. Moravec CS, Bond M. Calcium is released from the junctional sarcoplasmic reticulum during cardiac muscle contraction. Am J Physiol 1991;260:H989–H997. [PubMed: 2000992]
141. Moravec CS, Bond M. Effect of inotropic stimulation on mitochondrial calcium in cardiac muscle. J Biol Chem 1992;267:5310–5316. [PubMed: 1544913]
142. Morris K. Targeting the myocardial sodium-hydrogen exchange for treatment of heart failure. Expert Opin Ther Targets 2002;6:291–298. [PubMed: 12223070]
143. Neubauer S, Horn M, Cramer M, Harre K, Newell JB, Peters W, Pabst T, Ertl G, Hahn D, Ingwall JS, Kochsiek K. Myocardial phosphocreatine-to-ATP ratio is a predictor of mortality in patients with dilated cardiomyopathy. Circulation 1997;96:2190–2196. [PubMed: 9337189]
144. Ohata H, Chacon E, Tesfai SA, Harper IS, Herman B, Lemasters JJ. Mitochondrial Ca^{2+} transients in cardiac myocytes during the excitation-contraction cycle: effects of pacing and hormonal stimulation. J Bioenerg Biomembr 1998;30:207–222. [PubMed: 9733088]
145. Ohler A, Houser S, Tomaselli GF, O'Rourke B. Transverse tubules are unchanged in myocytes from failing human hearts. Biophys J 2001;80590e (abstract)
146. O'Rourke B, Kass DA, Tomaselli GF, Kaab S, Tunin R, Marban E. Mechanisms of altered excitation-contraction coupling in canine tachycardia-induced heart failure, I: experimental studies. Circ Res 1999;84:562–570. [PubMed: 10082478]
147. Pacher P, Csordas P, Schneider T, Hajnoczky G. Quantification of calcium signal transmission from sarco-endoplasmic reticulum to the mitochondria. J Physiol 2000;529(Pt 3):553–564. [PubMed: 11118489]

148. Pacher P, Thomas AP, Hajnoczky G. Ca^{2+} marks: miniature calcium signals in single mitochondria driven by ryanodine receptors. Proc Natl Acad Sci U S A 2002;99:2380–2385. [PubMed: 11854531]
149. Patterson SW, Piper H, Starling EH. The regulation of the heartbeat. J Physiol 1914;48:357–379. [PubMed: 16993262]
150. Paucek P, Jaburek M. Kinetics and ion specificity of $Na(^{+})/Ca(^{2+})$ exchange mediated by the reconstituted beef heart mitochondrial $Na(^{+})/Ca(^{2+})$ antiporter. Biochim Biophys Acta 2004;1659:83–91. [PubMed: 15511530]
151. Peskoff A, Langer GA. Calcium concentration and movement in the ventricular cardiac cell during an excitation-contraction cycle. Biophys J 1998;74:153–174. [PubMed: 9449319]
152. Peskoff A, Post JA, Langer GA. Sarcolemmal calcium binding sites in heart: II. Mathematical model for diffusion of calcium released from the sarcoplasmic reticulum into the diadic region. J Membr Biol 1992;129:59–69. [PubMed: 1404341]
153. Piacentino V 3rd, Weber CR, Chen X, Weisser-Thomas J, Margulies KB, Bers DM, Houser SR. Cellular basis of abnormal calcium transients of failing human ventricular myocytes. Circ Res 2003;92:651–658. [PubMed: 12600875]
154. Pieske B, Houser SR. $[Na^{+}]_{i}$ handling in the failing human heart. Cardiovasc Res 2003;57:874–886. [PubMed: 12650866]
155. Pieske B, Maier LS, Piacentino V 3rd, Weisser J, Hasenfuss G, Houser S. Rate dependence of $[Na^{+}]$i and contractility in nonfailing and failing human myocardium. Circulation 2002;106:447–453. [PubMed: 12135944]
156. Pogwizd SM, Sipido KR, Verdonck F, Bers DM. Intracellular Na in animal models of hypertrophy and heart failure: contractile function and arrhythmogenesis. Cardiovasc Res 2003;57:887–896. [PubMed: 12650867]
157. Reed KC, Bygrave FL. A low molecular weight ruthenium complex inhibitory to mitochondrial Ca^{2+} transport. FEBS Lett 1974;46:109–114. [PubMed: 4371774]
158. Rice JJ, Jafri MS, Winslow RL. Modeling gain and gradedness of Ca^{2+} release in the functional unit of the cardiac diadic space. Biophys J 1999;77:1871–1884. [PubMed: 10512809]
159. Rizzuto R, Duchen MR, Pozzan T. Flirting in little space: the ER/mitochondria Ca^{2+} liaison. Sci STKE. 20042004:re1
160. Rizzuto R, Pozzan T. Microdomains of intracellular Ca^{2+}: molecular determinants and functional consequences. Physiol Rev 2006;86:369–408. [PubMed: 16371601]
161. Robert V, Gurlini P, Tosello V, Nagai T, Miyawaki A, Di Lisa F, Pozzan T. Beat-to-beat oscillations of mitochondrial $[Ca^{2+}]$ in cardiac cells. Embo J 2001;20:4998–5007. [PubMed: 11532963]
162. Ruiz-Meana M, Garcia-Dorado D, Pina P, Inserte J, Agullo L, Soler-Soler J. Cariporide preserves mitochondrial proton gradient and delays ATP depletion in cardiomyocytes during ischemic conditions. Am J Physiol Heart Circ Physiol 2003;285:H999–H1006. [PubMed: 12915386]
163. Sabbah HN, Chandler MP, Mishima T, Suzuki G, Chaudhry P, Nass O, Biesiadecki BJ, Blackburn B, Wolff A, Stanley WC. Ranolazine, a partial fatty acid oxidation (pFOX) inhibitor, improves left ventricular function in dogs with chronic heart failure. J Card Fail 2002;8:416–422. [PubMed: 12528095]
164. Saks V, Dzeja P, Schlattner U, Vendelin M, Terzic A, Wallimann T. Cardiac system bioenergetics: metabolic basis of the Frank-Starling law. J Physiol 2006;571:253–273. [PubMed: 16410283]
165. Saks VA, Kuznetsov AV, Vendelin M, Guerrero K, Kay L, Seppet EK. Functional coupling as a basic mechanism of feedback regulation of cardiac energy metabolism. Mol Cell Biochem 2004;256'257:185–199.
166. Saupe KW, Spindler M, Tian R, Ingwall JS. Impaired cardiac energetics in mice lacking muscle-specific isoenzymes of creatine kinase. Circ Res 1998;82:898–907. [PubMed: 9576109]
167. Scaduto RC Jr, Grotyohann LW. 2,3-butanedione monoxime unmasks $Ca(^{2+})$-induced NADH formation and inhibits electron transport in rat hearts. Am J Physiol Heart Circ Physiol 2000;279:H1839–H1848. [PubMed: 11009471]
168. Scholz W, Albus U, Counillon L, Gogelein H, Lang HJ, Linz W, Weichert A, Scholkens BA. Protective effects of HOE642, a selective sodium-hydrogen exchange subtype 1 inhibitor, on cardiac ischaemia and reperfusion. Cardiovasc Res 1995;29:260–268. [PubMed: 7736504]

169. Schwinger RH, Bundgaard H, Muller-Ehmsen J, Kjeldsen K. The Na, K-ATPase in the failing human heart. Cardiovasc Res 2003;57:913–920. [PubMed: 12650869]

170. Sedova M, Dedkova EN, Blatter LA. Integration of rapid cytosolic Ca^{2+} signals by mitochondria in cat ventricular myocytes. Am J Physiol Cell Physiol 2006;291:C840–C850. [PubMed: 16723510]

171. Seguchi H, Ritter M, Shizukuishi M, Ishida H, Chokoh G, Nakazawa H, Spitzer KW, Barry WH. Propagation of Ca^{2+} release in cardiac myocytes: role of mitochondria. Cell Calcium 2005;38:1–9. [PubMed: 15993240]

172. Semb SO, Lunde PK, Holt E, Tonnessen T, Christensen G, Sejersted OM. Reduced myocardial Na^{+}, $K(^{+})$-pump capacity in congestive heart failure following myocardial infarction in rats. J Mol Cell Cardiol 1998;30:1311–1328. [PubMed: 9710800]

173. Sham JS, Song LS, Chen Y, Deng LH, Stern MD, Lakatta EG, Cheng H. Termination of Ca^{2+} release by a local inactivation of ryanodine receptors in cardiac myocytes. Proc Natl Acad Sci U S A 1998;95:15096–15101. [PubMed: 9844021]

174. Shannon TR, Wang F, Puglisi J, Weber C, Bers DM. A mathematical treatment of integrated Ca dynamics within the ventricular myocyte. Biophys J 2004;87:3351–3371. [PubMed: 15347581]

175. Shao Q, Ren B, Elimban V, Tappia PS, Takeda N, Dhalla NS. Modification of sarcolemmal Na^{+}-K^{+}-ATPase and Na^{+}/Ca^{2+} exchanger expression in heart failure by blockade of renin-angiotensin system. Am J Physiol Heart Circ Physiol 2005;288:H2637–H2646. [PubMed: 15681692]

176. Sharma VK, Ramesh V, Franzini-Armstrong C, Sheu SS. Transport of Ca^{2+} from sarcoplasmic reticulum to mitochondria in rat ventricular myocytes. J Bioenerg Biomembr 2000;32:97–104. [PubMed: 11768767]

177. Shen JX, Wang S, Song LS, Han T, Cheng H. Polymorphism of Ca^{2+} sparks evoked from in-focus Ca^{2+} release units in cardiac myocytes. Biophys J 2004;86:182–190. [PubMed: 14695261]

178. Sipido KR, Volders PG, Vos MA, Verdonck F. Altered Na/Ca exchange activity in cardiac hypertrophy and heart failure: a new target for therapy? Cardiovasc Res 2002;53:782–805. [PubMed: 11922890]

179. Sipido KR, Wier WG. Flux of Ca^{2+} across the sarcoplasmic reticulum of guinea-pig cardiac cells during excitation-contraction coupling. J Physiol 1991;435:605–630. [PubMed: 1770453]

180. Smets I, Caplanusi A, Despa S, Molnar Z, Radu M, VandeVen M, Ameloot M, Steels P. Ca^{2+} uptake in mitochondria occurs via the reverse action of the Na^{+}/Ca^{2+} exchanger in metabolically inhibited MDCK cells. Am J Physiol Renal Physiol 2004;286:F784–F794. [PubMed: 14665432]

181. Soeller C, Cannell MB. Estimation of the sarcoplasmic reticulum Ca^{2+} release flux underlying Ca^{2+} sparks. Biophys J 2002;82:2396–2414. [PubMed: 11964229]

182. Song LS, Guatimosim S, Gomez-Viquez L, Sobie EA, Ziman A, Hartmann H, Lederer WJ. Calcium biology of the transverse tubules in heart. Ann N Y Acad Sci 2005;1047:99–111. [PubMed: 16093488]

183. Song LS, Sham JS, Stern MD, Lakatta EG, Cheng H. Direct measurement of SR release flux by tracking 'Ca^{2+} spikes' in rat cardiac myocytes. J Physiol 1998;512(Pt 3):677–691. [PubMed: 9769413]

184. Song LS, Sobie EA, McCulle S, Lederer WJ, Balke CW, Cheng H. Orphaned ryanodine receptors in the failing heart. Proc Natl Acad Sci USA 2006;103:4305–4310. [PubMed: 16537526]

185. Song Q, Schmidt AG, Hahn HS, Carr AN, Frank B, Pater L, Gerst M, Young K, Hoit BD, McConnell BK, Haghighi K, Seidman CE, Seidman JG, Dorn GW 2nd, Kranias EG. Rescue of cardiomyocyte dysfunction by phospholamban ablation does not prevent ventricular failure in genetic hypertrophy. J Clin Invest 2003;111:859–867. [PubMed: 12639992]

186. Sparagna GC, Gunter KK, Sheu SS, Gunter TE. Mitochondrial calcium uptake from physiological-type pulses of calcium.A description of the rapid uptake mode. J Biol Chem 1995;270:27510–27515. [PubMed: 7499209]

187. Stanley WC, Recchia FA, Lopaschuk GD. Myocardial substrate metabolism in the normal and failing heart. Physiol Rev 2005;85:1093–1129. [PubMed: 15987803]

188. Starling RC, Hammer DF, Altschuld RA. Human myocardial ATP content and in vivo contractile function. Mol Cell Biochem 1998;180:171–177. [PubMed: 9546644]

189. Stromer H, de Groot MC, Horn M, Faul C, Leupold A, Morgan JP, Scholz W, Neubauer S. $Na(^{+})$/$H(^{+})$ exchange inhibition with HOE642 improves postischemic recovery due to attenuation of Ca

($^{2+}$) overload and prolonged acidosis on reperfusion. Circulation 2000;101:2749–2755. [PubMed: 10851214]

190. Studer R, Reinecke H, Bilger J, Eschenhagen T, Bohm M, Hasenfuss G, Just H, Holtz J, Drexler H. Gene expression of the cardiac Na($^{+}$)-Ca^{2+} exchanger in end-stage human heart failure. Circ Res 1994;75:443–453. [PubMed: 8062418]
191. Szalai G, Csordas G, Hantash BM, Thomas AP, Hajnoczky G. Calcium signal transmission between ryanodine receptors and mitochondria. J Biol Chem 2000;275:15305–15313. [PubMed: 10809765]
192. Taegtmeyer H. Cardiac metabolism as a target for the treatment of heart failure. Circulation 2004;110:894–896. [PubMed: 15326079]
193. Territo PR, French SA, Balaban RS. Simulation of cardiac work transitions, in vitro: effects of simultaneous Ca^{2+} and ATPase additions on isolated porcine heart mitochondria. Cell Calcium 2001;30:19–27. [PubMed: 11396984]
194. Territo PR, French SA, Dunleavy MC, Evans FJ, Balaban RS. Calcium activation of heart mitochondrial oxidative phosphorylation: rapid kinetics of mVO2, NADH, AND light scattering. J Biol Chem 2001;276:2586–2599. [PubMed: 11029457]
195. Territo PR, Mootha VK, French SA, Balaban RS. Ca($^{2+}$) activation of heart mitochondrial oxidative phosphorylation: role of the F(0)/F(1)-AT-Pase. Am J Physiol Cell Physiol 2000;278:C423–C435. [PubMed: 10666039]
196. Tian R, Halow JM, Meyer M, Dillmann WH, Figueredo VM, Ingwall JS, Camacho SA. Thermodynamic limitation for Ca^{2+} handling contributes to decreased contractile reserve in rat hearts. Am J Physiol 1998;275:H2064–H2071. [PubMed: 9843805]
197. Tian R, Ingwall JS. Energetic basis for reduced contractile reserve in isolated rat hearts. Am J Physiol 1996;270:H1207–H1216. [PubMed: 8967358]
198. Tian R, Nascimben L, Ingwall JS, Lorell BH. Failure to maintain a low ADP concentration impairs diastolic function in hypertrophied rat hearts. Circulation 1997;96:1313–1319. [PubMed: 9286964]
199. Tian R, Nascimben L, Kaddurah-Daouk R, Ingwall JS. Depletion of energy reserve via the creatine kinase reaction during the evolution of heart failure in cardiomyopathic hamsters. J Mol Cell Cardiol 1996;28:755–765. [PubMed: 8732503]
200. Trollinger DR, Cascio WE, Lemasters JJ. Mitochondrial calcium transients in adult rabbit cardiac myocytes: inhibition by ruthenium red and artifacts caused by lysosomal loading of Ca($^{2+}$)-indicating fluorophores. Biophys J 2000;79:39–50. [PubMed: 10866936]
201. Trollinger DR, Cascio WE, Lemasters JJ. Selective loading of Rhod 2 into mitochondria shows mitochondrial Ca^{2+} transients during the contractile cycle in adult rabbit cardiac myocytes. Biochem Biophys Res Commun 1997;236:738–742. [PubMed: 9245725]
202. Undrovinas AI, Belardinelli L, Undrovinas NA, Sabbah HN. Ranolazine improves abnormal repolarization and contraction in left ventricular myocytes of dogs with heart failure by inhibiting late sodium current. J Cardiovasc Electrophysiol 2006;17(Suppl 1):S169–S177. [PubMed: 16686675]
203. Undrovinas AI, Maltsev VA, Kyle JW, Silverman N, Sabbah HN. Gating of the late Na^{+} channel in normal and failing human myocardium. J Mol Cell Cardiol 2002;34:1477–1489. [PubMed: 12431447]
204. Undrovinas AI, Maltsev VA, Sabbah HN. Repolarization abnormalities in cardiomyocytes of dogs with chronic heart failure: role of sustained inward current. Cell Mol Life Sci 1999;55:494–505. [PubMed: 10228563]
205. Valdivia CR, Chu WW, Pu J, Foell JD, Haworth RA, Wolff MR, Kamp TJ, Makielski JC. Increased late sodium current in myocytes from a canine heart failure model and from failing human heart. J Mol Cell Cardiol 2005;38:475–483. [PubMed: 15733907]
206. Verdonck F, Volders PG, Vos MA, Sipido KR. Increased Na^{+} concentration and altered Na/K pump activity in hypertrophied canine ventricular cells. Cardiovasc Res 2003;57:1035–1043. [PubMed: 12650881]
207. Verdonck F, Volders PG, Vos MA, Sipido KR. Intracellular Na^{+} and altered Na^{+} transport mechanisms in cardiac hypertrophy and failure. J Mol Cell Cardiol 2003;35:5–25. [PubMed: 12623296]

208. Weber CR, Ginsburg KS, Philipson KD, Shannon TR, Bers DM. Allosteric regulation of Na/Ca exchange current by cytosolic Ca in intact cardiac myocytes. J Gen Physiol 2001;117:119–131. [PubMed: 11158165]

209. Weber CR, Piacentino V 3rd, Ginsburg KS, Houser SR, Bers DM. Na($^{+}$)-Ca($^{2+}$) exchange current and submembrane [Ca($^{2+}$)] during the cardiac action potential. Circ Res 2002;90:182–189. [PubMed: 11834711]

210. Weber CR, Piacentino V 3rd, Houser SR, Bers DM. Dynamic regulation of sodium/calcium exchange function in human heart failure. Circulation 2003;108:2224–2229. [PubMed: 14557358]

211. Weiss RG, Gerstenblith G, Bottomley PA. ATP flux through creatine kinase in the normal, stressed, and failing human heart. Proc Natl Acad Sci USA 2005;102:808–813. [PubMed: 15647364]

212. Weisser-Thomas J, Piacentino V 3rd, Gaughan JP, Margulies K, Houser SR. Calcium entry via Na/Ca exchange during the action potential directly contributes to contraction of failing human ventricular myocytes. Cardiovasc Res 2003;57:974–985. [PubMed: 12650875]

213. Wendt-Gallitelli MF, Isenberg G. Total and free myoplasmic calcium during a contraction cycle: x-ray microanalysis in guinea-pig ventricular myocytes. J Physiol 1991;435:349–372. [PubMed: 1770441]

214. White RL, Wittenberg BA. Effects of calcium on mitochondrial NAD(P)H in paced rat ventricular myocytes. Biophys J 1995;69:2790–2799. [PubMed: 8599685]

215. White RL, Wittenberg BA. NADH fluorescence of isolated ventricular myocytes: effects of pacing, myoglobin, and oxygen supply. Biophys J 1993;65:196–204. [PubMed: 8369428]

216. Williamson JR, Ford C, Illingworth J, Safer B. Coordination of citric acid cycle activity with electron transport flux. Circ Res 1976;38:I39–I51. [PubMed: 1269091]

217. Winslow RL, Rice J, Jafri S, Marban E, O'Rourke B. Mechanisms of altered excitation-contraction coupling in canine tachycardia-induced heart failure, II: model studies. Circ Res 1999;84:571–586. [PubMed: 10082479]

218. Xie Z. Molecular mechanisms of Na/K-ATPase-mediated signal transduction. Ann N Y Acad Sci 2003;986:497–503. [PubMed: 12763870]

219. Xu KY, Zweier JL, Becker LC. Functional coupling between glycolysis and sarcoplasmic reticulum Ca^{2+} transport. Circ Res 1995;77:88–97. [PubMed: 7788886]

220. Yoshikane H, Nihei T, Moriyama K. Three-dimensional observation of intracellular membranous structures in dog heart muscle cells by scanning electron microscopy. J Submicrosc Cytol 1986;18:629–636. [PubMed: 3783792]

221. Zhou Z, Bers DM. Time course of action of antagonists of mitochondrial Ca uptake in intact ventricular myocytes. Pflugers Arch 2002;445:132–138. [PubMed: 12397397]

222. Zhou Z, Matlib MA, Bers DM. Cytosolic and mitochondrial Ca^{2+} signals in patch clamped mammalian ventricular myocytes. J Physiol 1998;507(Pt 2):379–403. [PubMed: 9518700]

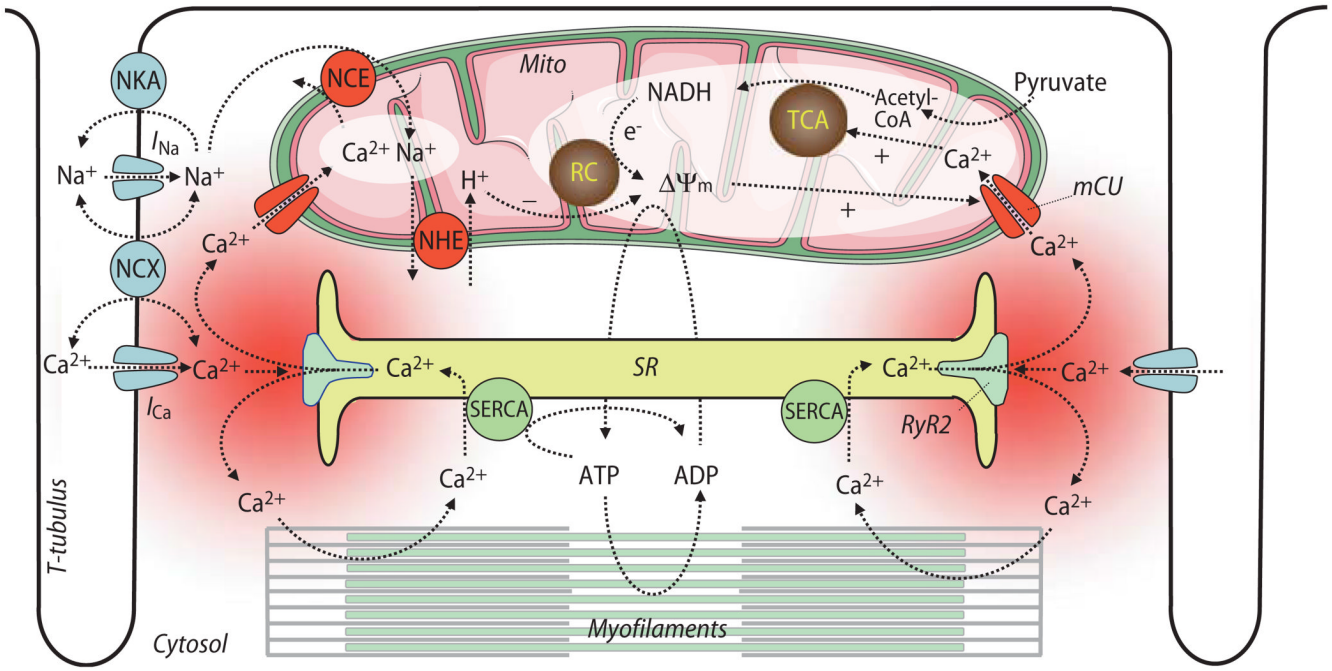

Fig. 1.

Overview on processes of excitation-contraction coupling and mitochondrial energetics. *SR* sarcoplasmic reticulum; *SERCA* SR Ca^{2+} ATPase; *Mito* mitochondria; *TCA* tricarboxylic acid cycle; *RC* respiratory chain; $\Delta\psi_m$ mitochondrial membrane potential; *NCE* mitochondrial Na^+/Ca^{2+}-exchanger; *NHE* mitochondrial Na^+/H^+ -exchanger; *NKA* sarcolemmal Na^+/K^+-ATPase; *NCX* sarcolemmal Na^+/Ca^{2+}-exchanger; *RyR2* ryanodine receptor type 2; *mCU* mitochondrial Ca^{2+}-uniporter; I_{Na} and I_{Ca}, currents of voltage-gated Na^+- or Ca^{2+}-channels, respectively

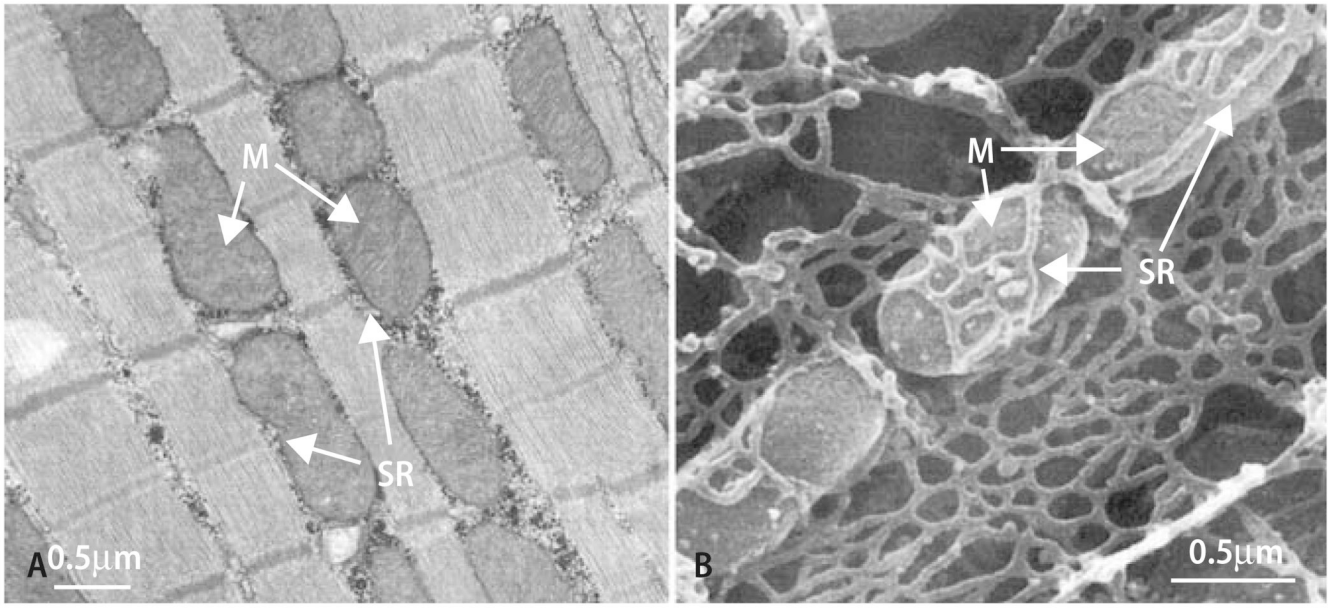

Fig. 2.
Longitudinal (**A**) or scanning (**B**) electron micrographs of cardiac myocytes. *M* mitochondria; *SR* sarcoplasmic reticulum. With permission from Territo et al. [194] and Yoshikane et al. [220], respectively

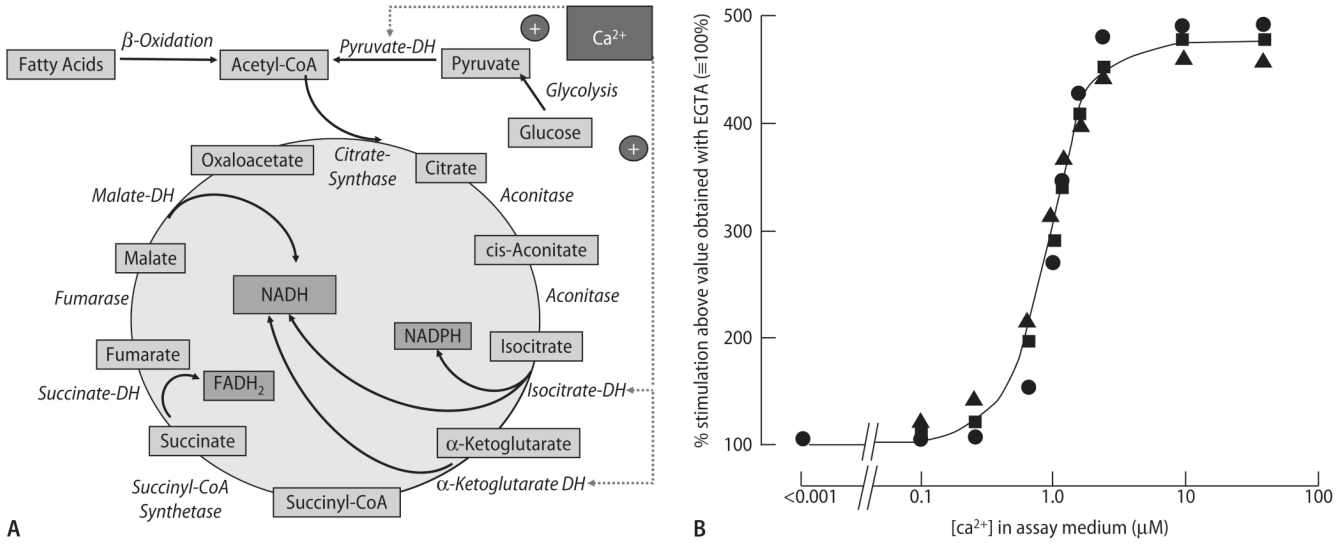

Fig. 3.

(**A**) Enzymatic reactions of the tricarboxylic acid (TCA) cycle, and their regulation by Ca^{2+}. *DH* dehydrogenase. (**B**) Stimulation of pyruvate-dehydrogenase phosphatase (PDH-PPase), NAD-isocitrate dehydrogeNase (NAD-ICDH) and α-ketoglutarate dehydrogenase (α-KGDH) enzymatic activity by Ca^{2+} in extracts of mitochondria. Activity in the presence of EGTA was ~ 10–20% of maximal velocity (V_{max}), respectively. Reproduced from Denton & McCormack [54] with permission

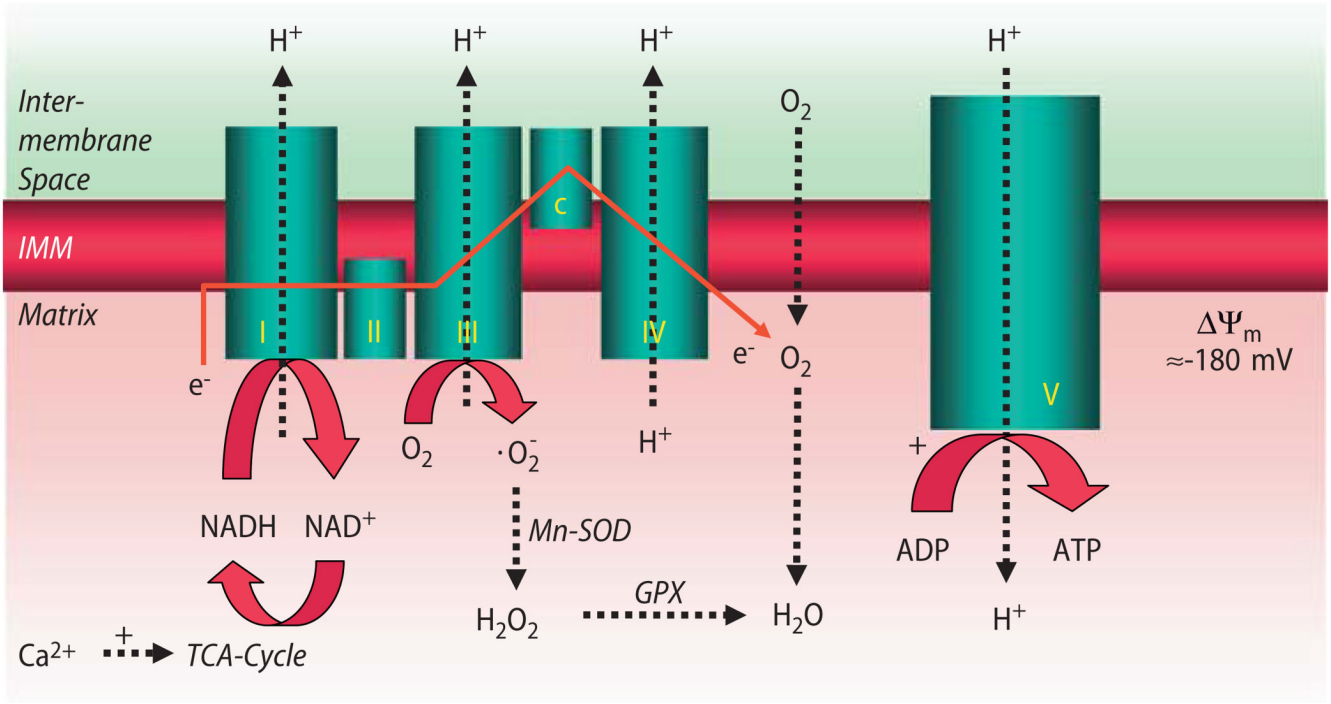

Fig. 4.

Processes of oxidative phosphorylation at the mitochondrial respiratory chain. *I–V* complexes I–V of the respiratory chain. *Complex V* F_1/F_0-ATPase; *c* cytochrome c. Electrons (e^-) donated by NADH to complex I (and by succinate to complex II; not shown) elicit sequential redox reactions at complexes I–IV, promoting H^+-translocation from the matrix to the intermembrane space across the inner mitochondrial membrane (IMM). This creates a proton gradient (ΔpH), which together with the electrochemical gradient ($\Delta\psi_m$) constitutes the driving force for protons to flow back into the matrix space via F_1/F_0-ATPase, promoting ATP-production from ADP. At complex III (and I; not shown), the superoxide anion radical is produced already under physiological conditions. It is dismutated to hydrogen peroxide (H_2O_2) by Mn^{2+}-dependent superoxide-dismutase (Mn-SOD), which is eliminated to H_2O by glutathione-peroxidase (GPX). While Ca^{2+} activates (+) TCA-cycle dehydrogenases (but also complex V of the respiratory chain; not shown), ADP regulates respiration by increasing complex V activity (+)

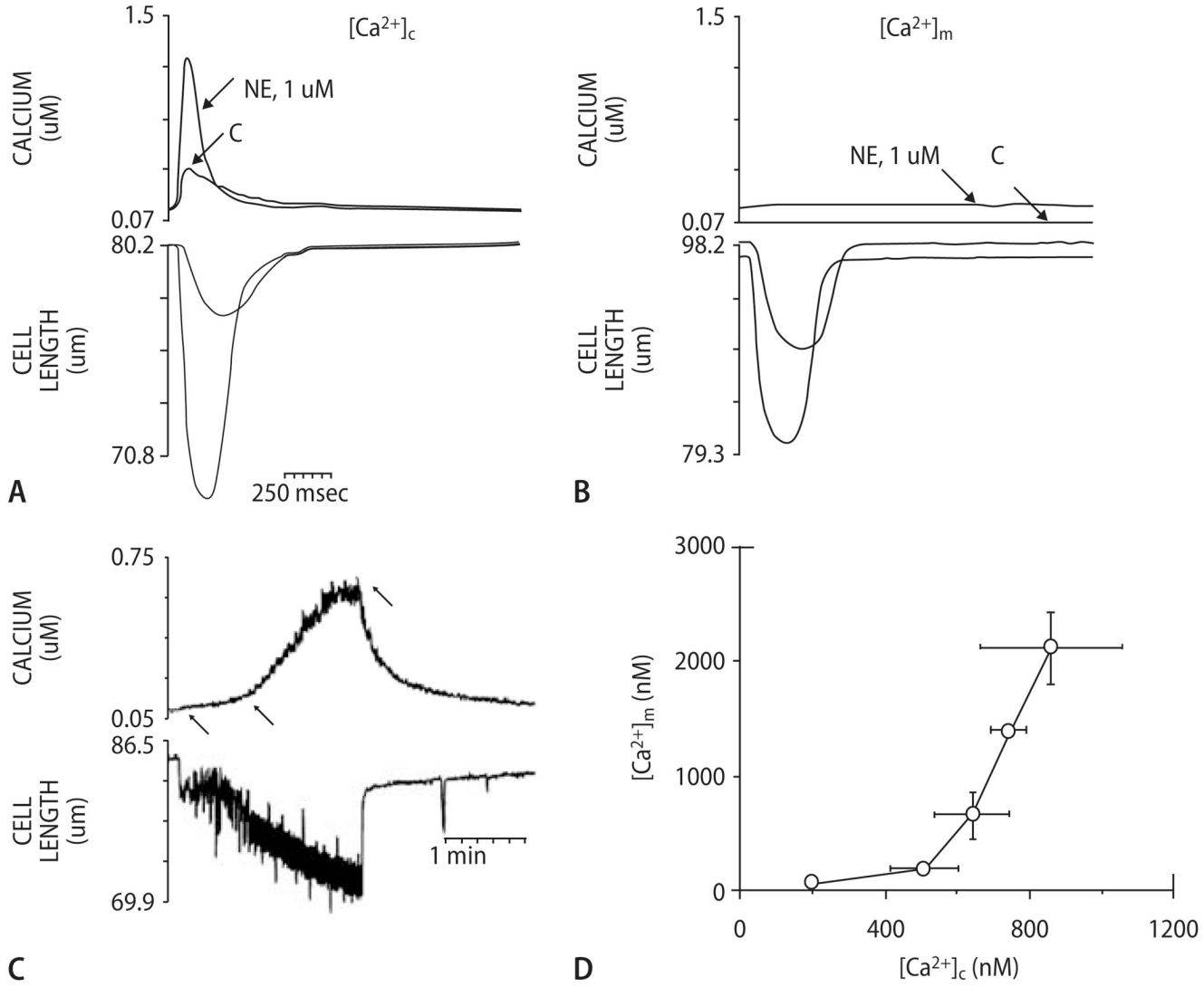

Fig. 5.

$[Ca^{2+}]_c$ and $[Ca^{2+}]_m$ during a single contraction in the presence and absence of norepinephrine (NE): myocyte loaded with indo-1/salt (**A**); myocyte loaded with indo-1/AM and quenched with Mn^{2+} (**B**). A and B each show results from a single cell, stimulated at steady-state 0.2 Hz in presence and absence of 1 μM NE. It is seen that there is no response of $[Ca^{2+}]_m$ to a single electrical stimulation. (**C**) Kinetics of rise and fall of $[Ca^{2+}]_m$ in response to changed pacing rate. Top: $[Ca^{2+}]_m$ for a single myocyte, superfused with medium containing 1 μM NE; bottom: mechanical response of cell to electrical stimulation. At 1st arrow, stimulation frequency was increased from 0 to 4 Hz; at 2nd arrow, cell begins to contract in synchrony with 4 Hz stimulation; at 3rd arrow, pacing was discontinued. (**D**) Relation between $[Ca^{2+}]_m$ and mean $[Ca^{2+}]_c$ during Na^+-replacement experiments with slow cytosolic and mitochondrial Ca^{2+} uptake. Reproduced with permission from Miyata et al. [137]

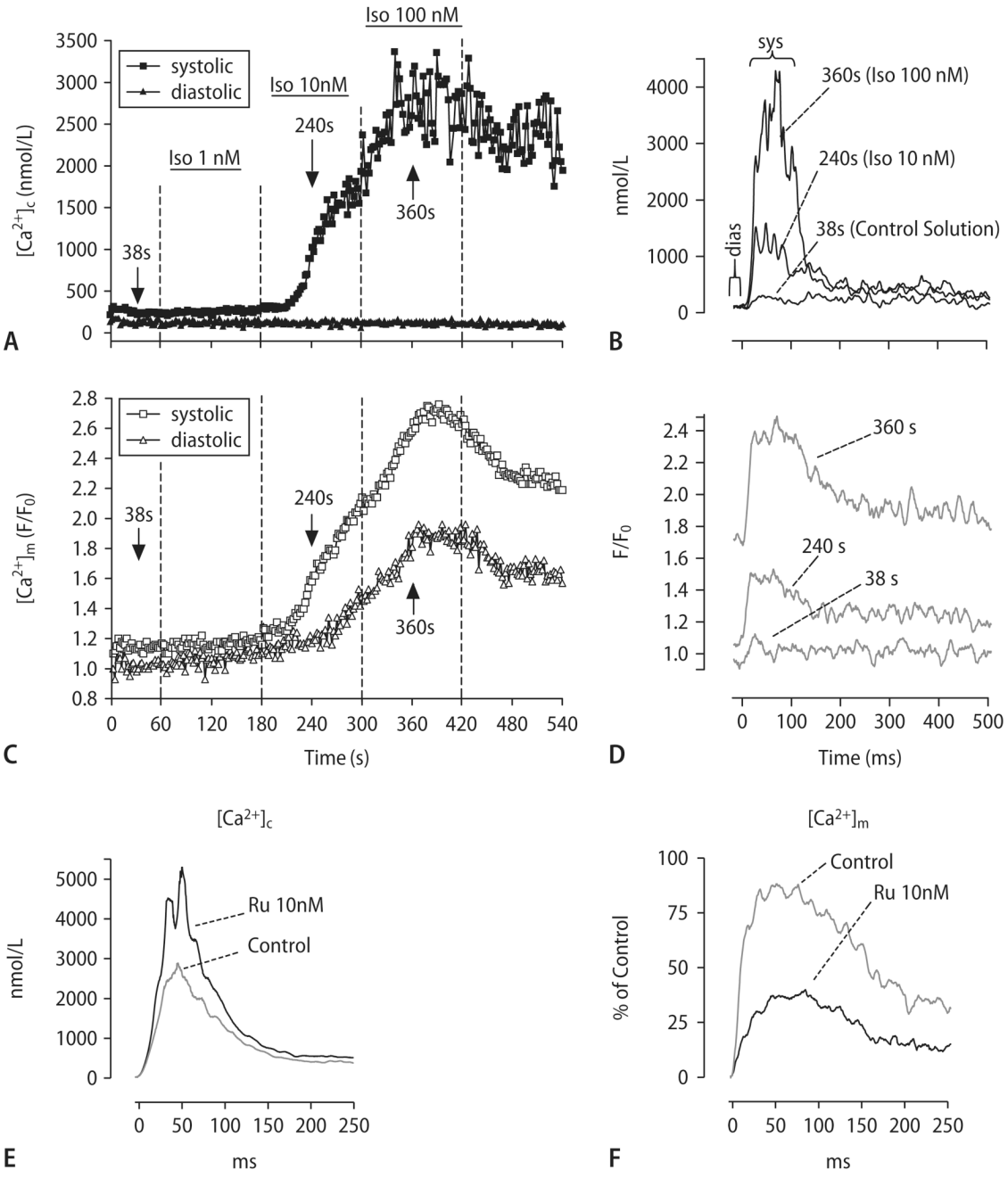

Fig. 6.

(**A-D**) Representative experiment determining $[Ca^{2+}]_c$ and $[Ca^{2+}]_m$ in the same cell. $[Ca^{2+}]_c$ transients were elicited at 1 Hz in the absence and presence of isoproterenol (Iso, 1–100 nmol/L; (**A**), (**C**)). The $[Ca^{2+}]$ transients in (**B**) and (**D**) were recorded at the indicated time points of the protocol (arrows in (**A**), (**C**)). (**E**) and (**F**) Cytosolic (**E**) and mitochondrial Ca^{2+}-transients (**F**) in the absence and presence of Ru360 (10 nmol/L)

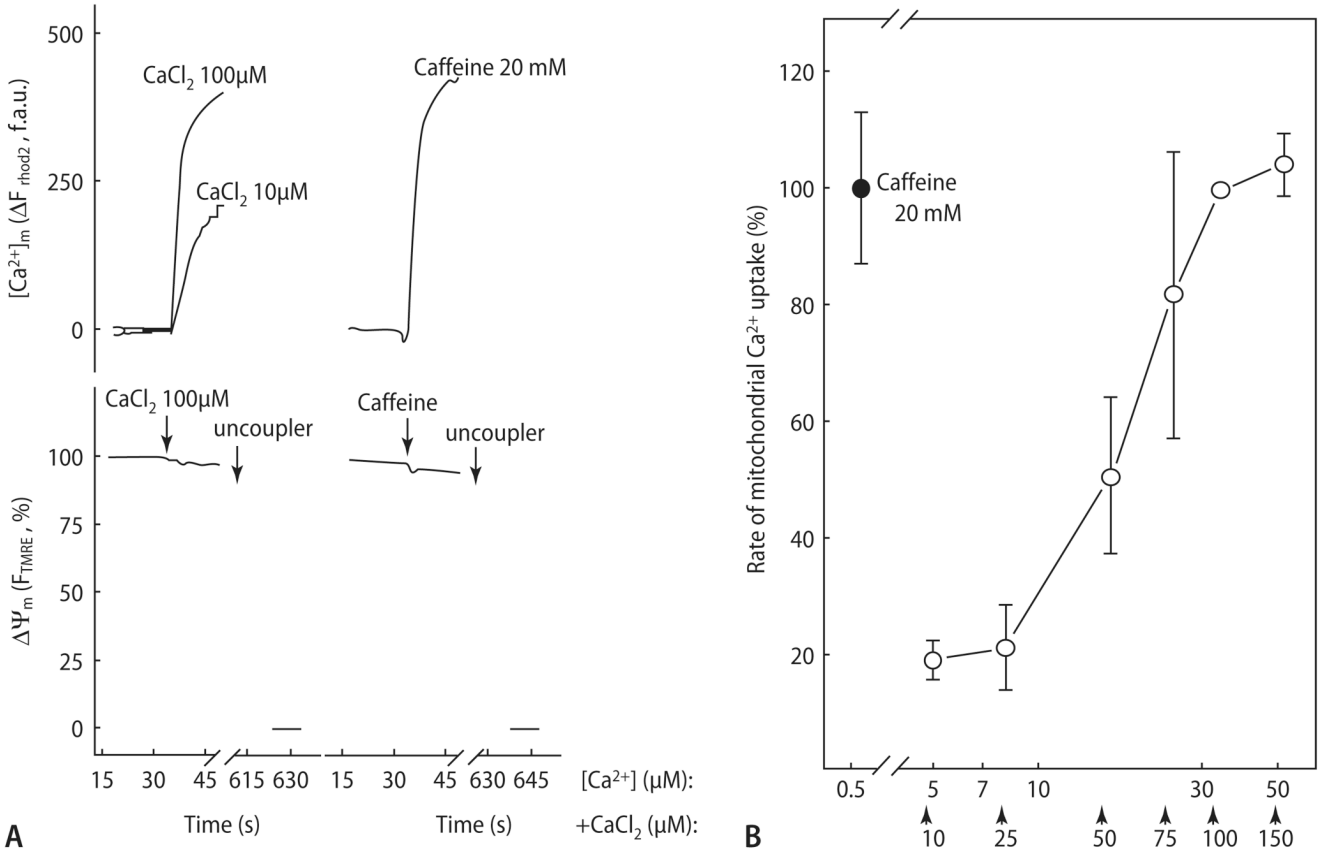

Fig. 7.

Full activation of mitochondrial Ca^{2+} uptake during RyR-mediated Ca^{2+} release. (**A**) Ca^{2+}- and caffeine induced $[Ca^{2+}]_m$ and $\Delta\psi_m$ responses were measured in permeabilized myotubes using rhod-2 and TMRM, respectively. Uncoupler (1 µM CCCP and 2.5 µg/ml oligomycin) was added as indicated. (**B**) The rate of mitochondrial Ca^{2+} uptake was measured at varying $[Ca^{2+}]$ obtained by the addition of $CaCl_2$ in adherent rhod-2 loaded permeabilized cells. The added $CaCl_2$ concentration values are indicated with arrows below the x axis, and the effective $[Ca^{2+}]_c$ were calculated. To prevent Ca^{2+}-induced Ca^{2+}-release via RyR2, the cells were preincubated with thapsigargin to inhibit the SR Ca^{2+} ATPase and hence to deplete the SR prior to Ca^{2+} addition. Reproduced from Szalai et al. [191] with permission

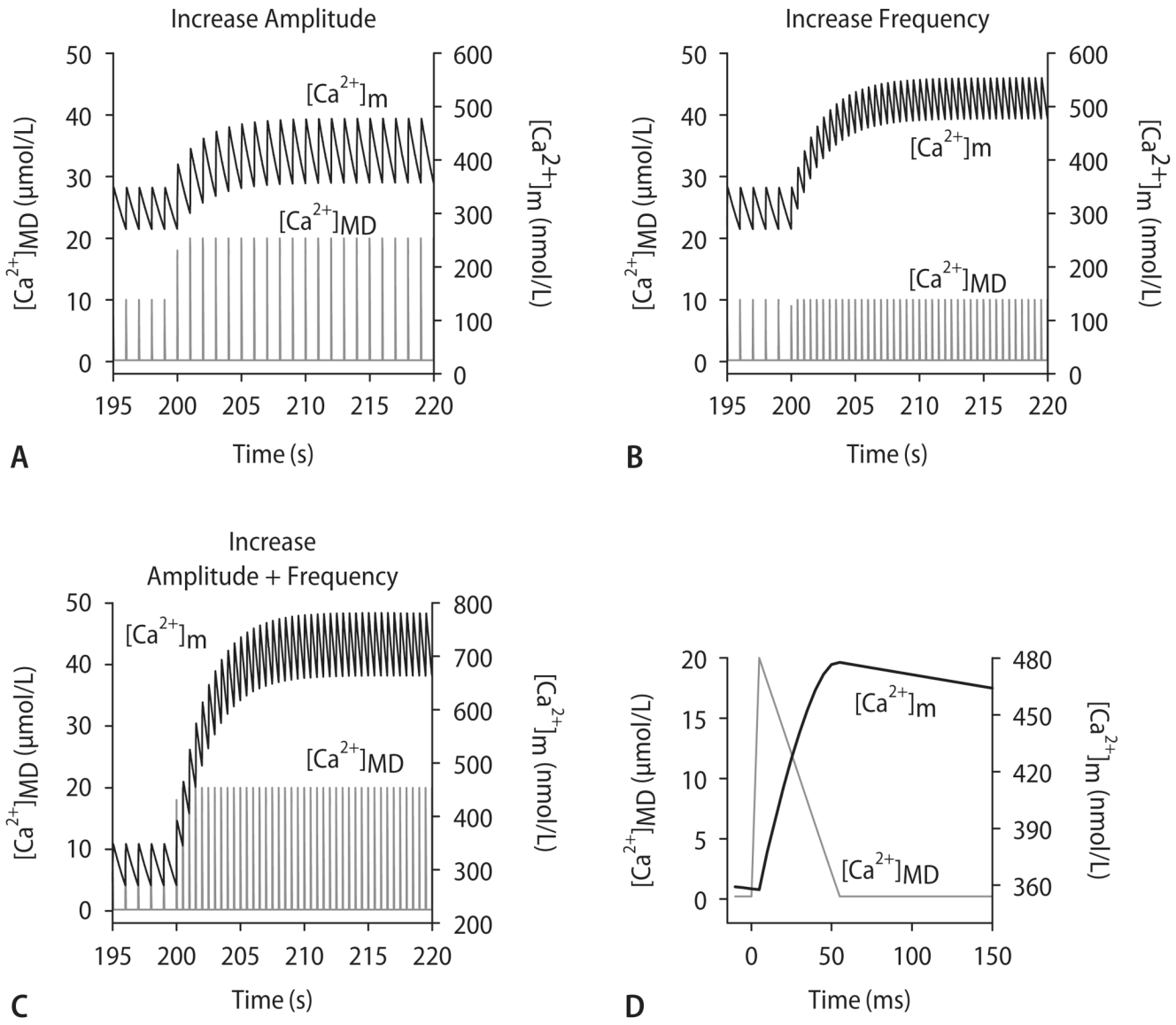

Fig. 8.

Computational modeling of $[Ca^{2+}]_m$, assuming a microdomain (MD) in which mitochondria are exposed to $[Ca^{2+}]$ pulses of 10–20 µmol/L for 50 ms (**D**; representative pulse taken from t = 215 s in **A**). Starting from steady-state conditions with $[Ca^{2+}]_{MD}$ oscillating from 0.1 to 10 µmol/L at 1 Hz, an increase of amplitude (**A**, from 10 to 20 µmol/L), frequency (**B**, from 1 to 2 Hz) or both (**C**) of $[Ca^{2+}]_{MD}$ transients were simulated. Reproduced from Maack et al. [117] with permission

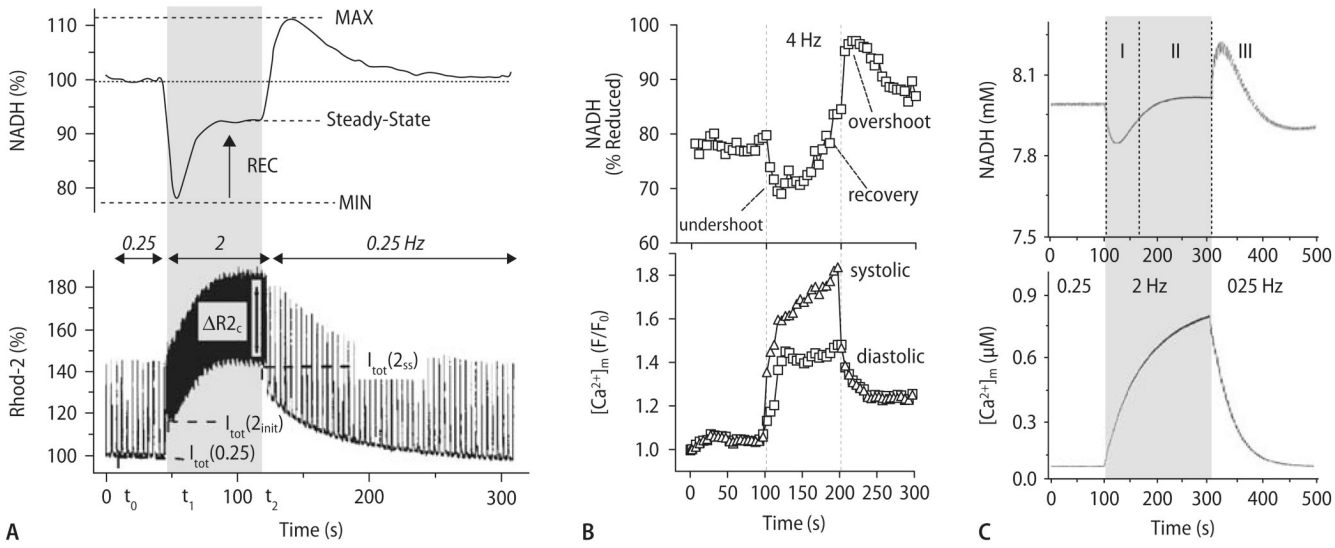

Fig. 9.

Time-dependent behavior of $[Ca^{2+}]_m$ and NADH after changes in workload. (**A**) Experimental data showing the responses of NADH (upper panel) and $[Ca^{2+}]_m$ (lower panel) to an increase in stimulation frequency from 0.5 to 2 Hz in a rat cardiac trabecula. (**B**) NADH (upper panel) and $[Ca^{2+}]_m$ (lower panel) in response to an increase of stimulation frequency from 0 to 4 Hz in the presence of isoproterenol (100 nM). (**C**) Computational modeling of NADH and $[Ca^{2+}]_m$ by integrating the kinetics of EC coupling, mitochondrial Ca^{2+} transporters and energetics in response to a change in stimulation frequency from 0.25 Hz to 2 Hz (for parameters, see [46]). I, undershoot; II, recovery, and III, overshoot of NADH. Reproduced from Brandes and Bers (**A**; [26]), Maack et al. (**B**; [117]) and Cortassa et al. (C; [46]) with permission

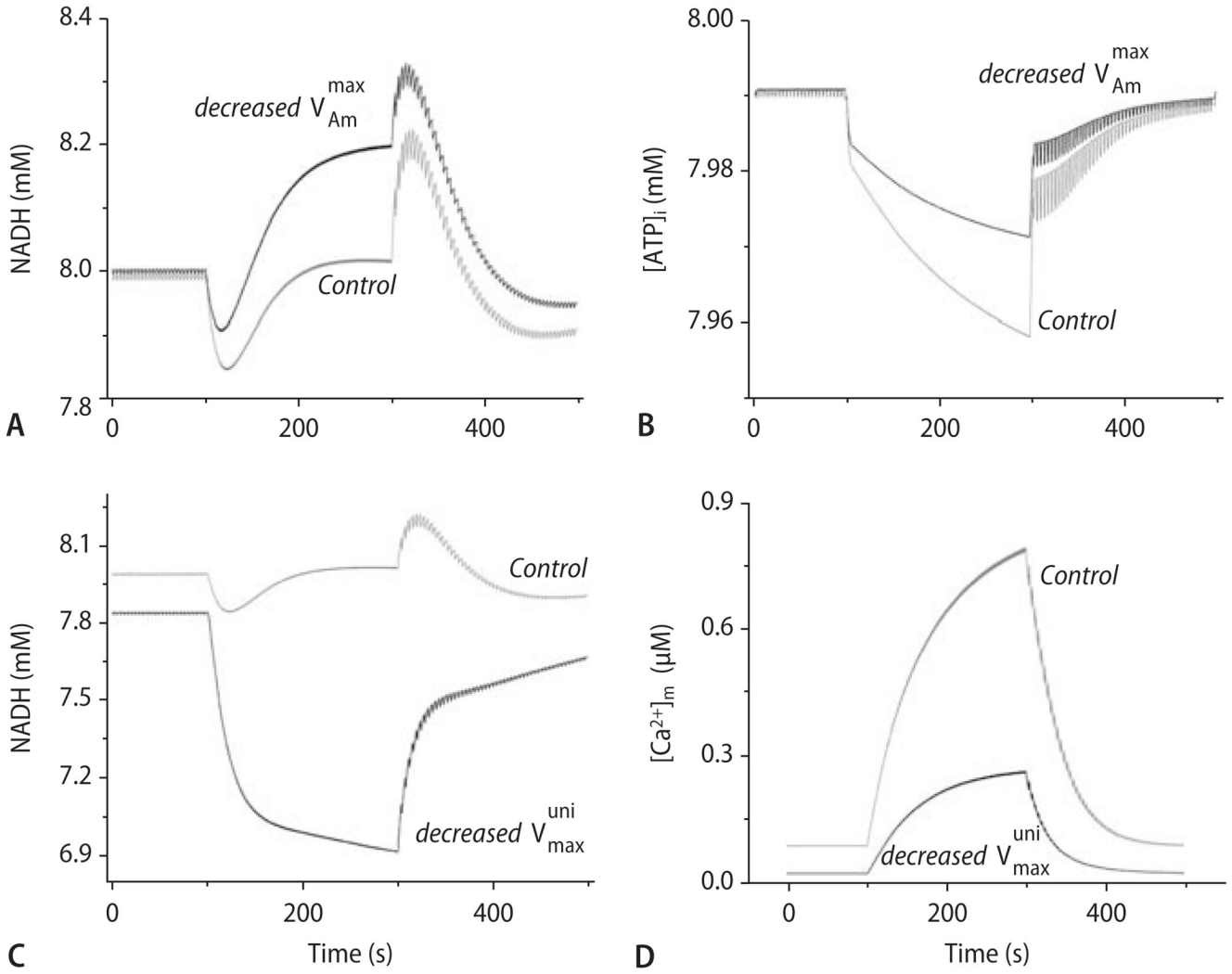

Fig. 10.

Effect of changing the actomyosin- (AM-) ATPase and mCU on the computational model (described by Cortassa et al. [46]; compare Fig. 9C) on energetic behavior after changes in workload. (**A**) The behavior of NADH with the maximal rate of ATP hydrolysis by the AM-ATPase being decreased to onehalf (solid trace; $V_{max/AM} = 3.6 \cdot 10^{-3}$ mM ms^{-1}) of the control value (shaded trace). (**B**) The profile of average ATP_i for changes in workload under control conditions (shaded trace) or with decreased AM-ATPase activity (solid trace). (**C**) The NADH profile with the maximal rate of the mCU decreased to $1/10^{th}$ (solid trace; $V_{max/mCU} = 2.75 \cdot 10^{-3}$ mM ms^{-1}) of the control value (shaded trace). (**D**) The profile of $[Ca^{2+}]_m$ accumulation for the low mCU condition described in (**C**) (solid trace) as compared to the control (shaded trace). Reproduced from Cortassa et al. [46] with permission

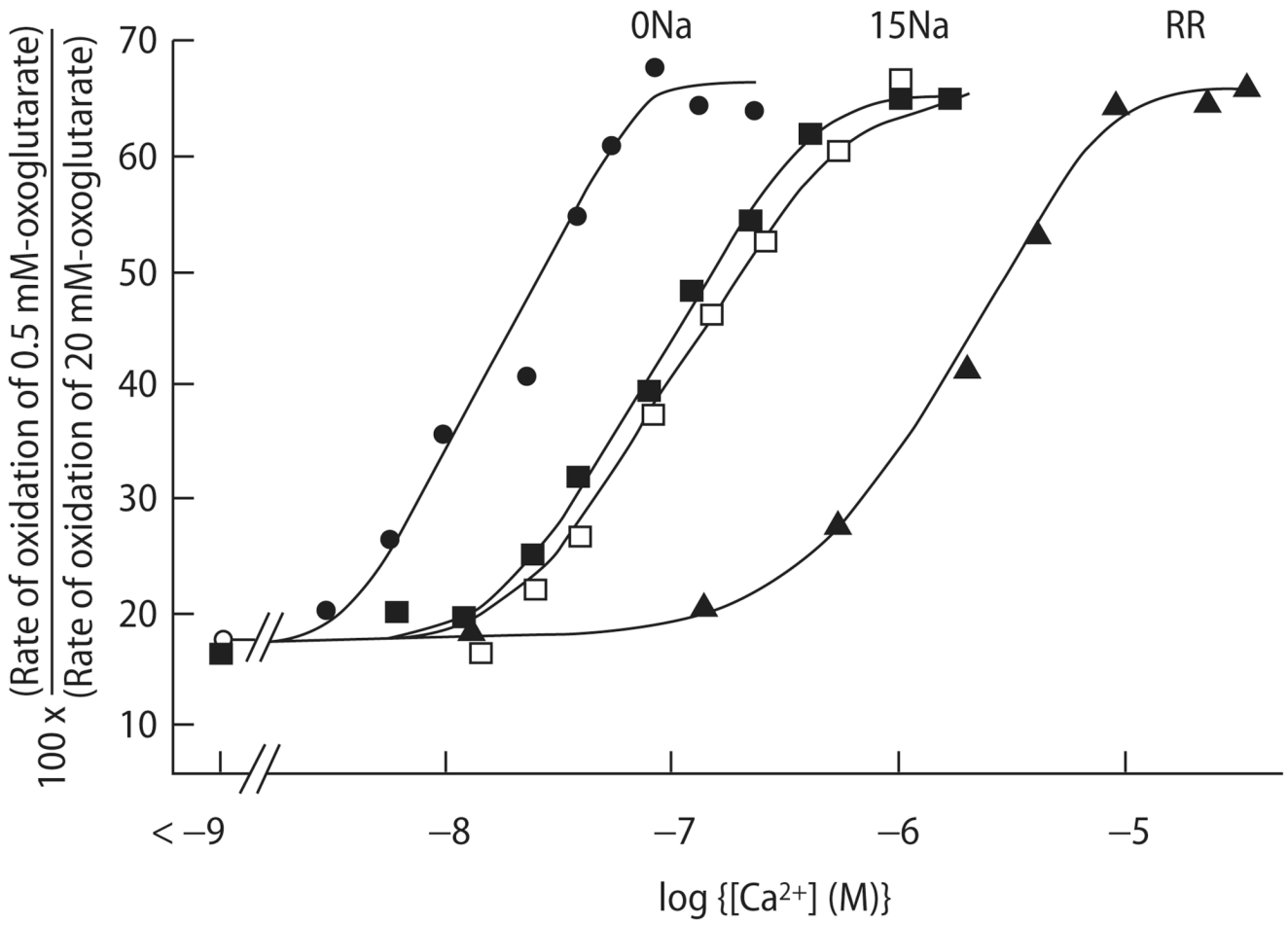

Fig. 11.
Stimulation of α-ketoglutarate oxidation by Ca^{2+} in the absence and presence of Na^{+} (15 mM) and the mCU-inhibitor ruthenium red (RR). Reproduced from Denton et al. [55] with permission

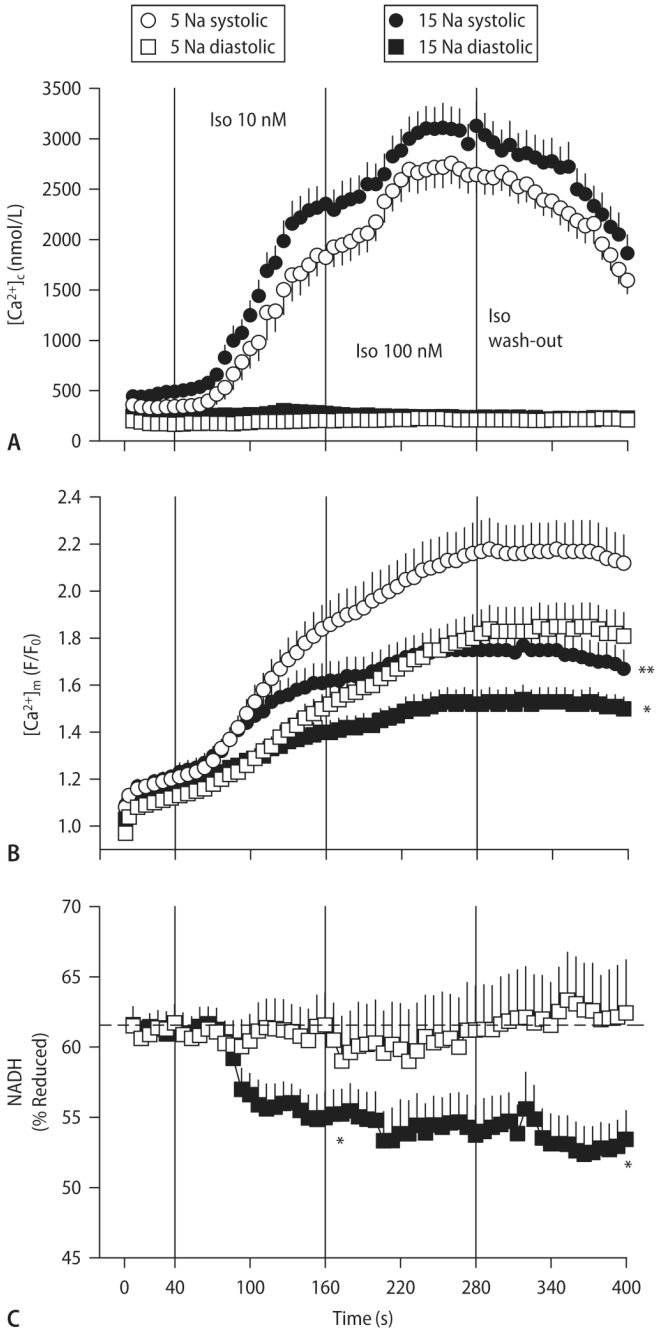

Fig. 12.

$[Ca^{2+}]_c$ (**A**), $[Ca^{2+}]_m$ (**B**) and reduced NADH (**C**) in guinea-pig cardiac myocytes paced at 3 Hz and exposure to 10 and 100 nM isoproterenol, with either 5 or 15 mM $[Na^+]$ in the pipet. Reproduced from Maack et al. [117] with permission

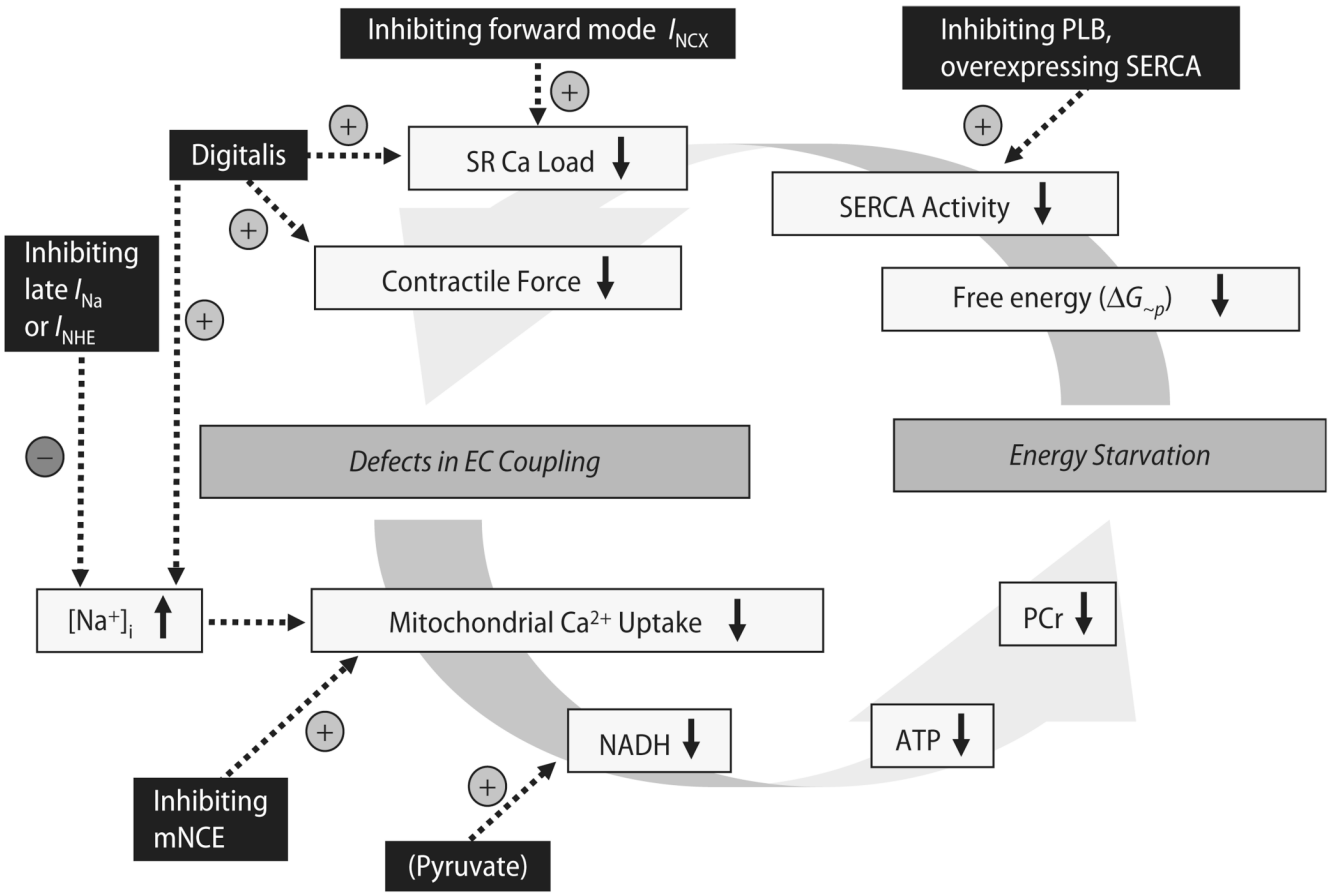

Fig. 13.
Hypothetical vicious cycle (and potential targets for therapeutic interventions) of defects in EC coupling and energy depletion in chronic heart failure. PCr phosphocreatine; PLB phospholamban; SERCA SR Ca^{2+}-ATPase